

Deformational styles in a sequence of olistostromal mélanges, Pacific Rim Complex, western Vancouver Island, Canada

MARK T. BRANDON *Department of Geology and Geophysics, Yale University, Box 6666, New Haven, Connecticut 06511*

ABSTRACT

The Pacific Rim Complex is exposed in a fault-bounded slice along the west coast of Vancouver Island. It is divided into two parts: (1) the Ucluth Formation, a basement unit composed of lower Mesozoic arc-volcanic rocks, and (2) a suprajacent sedimentary sequence, more than 2 km thick, composed of Lower Cretaceous olistostromal mélanges. An unconformity is present, at least locally, at the Ucluth-mélange contact and indicates that the Ucluth Formation is stratigraphic basement to the mélanges.

Mélange-style deformation is restricted to the sedimentary sequence and has affected virtually all parts of that sequence. The mélanges formed without the development of a cleavage or pervasive cataclasis, indicating that deformation occurred prior to consolidation of the sediments.

Three types of mélanges have been recognized. The first consists of a matrix of interbedded mudstone, chert, sandstone, and green tuff, which encloses numerous exotic blocks of igneous rocks and limestone. Beds within the matrix show variable amounts of layer-parallel fragmentation, which is attributed to *in situ* liquefaction and lateral flowage within individual beds. The blocks in this mélange, most of which were derived from the underlying Ucluth Formation, are considered to be submarine slide blocks, produced by rock falls from nearby basement scarps. The matrix sediments near the blocks commonly contain wispy lenses of poorly sorted plutonic and volcanic detritus ("green tuff"), interpreted as scree from the rock slides.

The second and third types of mélange are distinguished by the predominance of either mudstone or sandstone but are otherwise quite similar. These mélanges lack exotic blocks and consist of a contorted assemblage of mudstone, turbidite sandstone, conglomer-

ate, pebbly mudstone, and rare chert, all of which are depositionally interrelated. Sedimentary structures and stratal coherence are generally well preserved. The internal structure of these mélanges consists of a series of dismembered depositional sequences. Individual sequences are commonly more than 75 m thick. Some are upright and others are overturned. Paleocological evidence indicates that some of these sequences were originally deposited in an intra-slope basin. Thus, these mélanges are interpreted to have formed mainly by the accumulation of large slump sheets at the base of a submarine slope.

Previous interpretations have considered the Pacific Rim Complex to be a late Mesozoic subduction complex constructed along the western margin of the Wrangellia terrane (Vancouver Island). Several factors argue against a subduction-mélange interpretation. (1) The mélanges were deposited on an older, arc-related basement, not oceanic crust; (2) exotic blocks were introduced as rock slides and not by subsurface faulting; and (3) at least some of the strata originated in an intra-slope basin. The heterogeneous deformational style is more compatible with an origin by near-surface mass-movement processes, including submarine slides, rock falls, debris flows, and *in situ* liquefaction. The amount of mass wasting recorded in the Pacific Rim mélanges probably requires a seismically active setting, where frequent ground shaking produced large transients in pore fluid pressure.

Similarities in stratigraphy and metamorphism suggest that during Late Cretaceous time, the Pacific Rim Complex was part of the San Juan-Cascades thrust system, located 220 km to the southeast in northwestern Washington State. If this is correct, the Pacific Rim mélanges would have formed on the inboard side of Wrangellia, about 30 m.y. prior to the collision of Wrangellia with the

American continent. The present location of the Pacific Rim, outboard of Wrangellia, is attributed to younger (latest Cretaceous or early Tertiary) transcurrent displacement.

INTRODUCTION

The Pacific Rim Complex comprises Mesozoic mélanges and volcanic rocks, exposed in a narrow fault-bounded slice, about 60 km long, along the west coast of Vancouver Island (Figs. 1 and 2). The unit was first studied by Muller (1973, 1977a) and Page (1974), who concluded that it was a late Mesozoic subduction complex. The prevailing view now is that the Pacific Rim Complex is a remnant of a once-continuous subduction complex that fringed western North America during the late Mesozoic (Dickinson, 1976; Muller, 1977a; Jones and others, 1977). Correlative units would include the Franciscan Complex of California and southern Oregon, and the Chugach terrane of southern Alaska (Fig. 1).

An important objective of my work in the Pacific Rim Complex (Brandon, 1984, 1985) was to re-examine the subduction interpretation. Previous workers mapped the unit only in reconnaissance (Muller, 1973, 1976; Page, 1974; Muller and others, 1981). As part of my study, I mapped 85% of the complex (Fig. 3) at a scale of 1:24,000 or larger. The west side of the Ucluth Peninsula (Fig. 4) was mapped at 1:6,000. Considerable effort was directed toward determining the age and origin of the various components of the mélange units, using fossil data, depositional facies, and chemical analyses of igneous rocks.

This paper focuses specifically on the sediment-rich mélanges that make up a large part of the Pacific Rim Complex; a companion paper (Brandon, 1989a) considers the origin of associated igneous rocks. The Pacific Rim is ideally suited for these studies. Pleistocene glaciation and frequent Pacific storms have produced extensive tracts of fresh coastal outcrop, which permit detailed mapping of the mélanges, in-

Additional material for this article (an appendix) may be obtained free of charge by requesting Supplementary Data 8916 from the GSA Documents Secretary.

cluding their internal structure, block-matrix relationships, and external contacts. Furthermore, the very low metamorphic grade of the Pacific Rim mélanges and the general absence of superposed deformation allow fabrics and structures to be interpreted with more confidence than is possible in many other mélangé terranes.

The term "mélangé" is used herein in a purely descriptive sense. It indicates a large (>~100 m thick) body of rock composed mainly of sedimentary materials and typified either by a general lack of internal stratal continuity or by blocks of various sizes and shapes dispersed in a finer-grained sedimentary matrix (after Cowan, 1985). Typical matrix materials include mudstone, sandstone, and in some cases detrital serpentine. Blocks may be derived from either local (native) or extraformational (exotic) sources. Note that as used herein, the term "mélangé" refers exclusively to sediment-rich units and excludes serpentine-rich shear zones or matrix-poor fault zones (Type IV mélangé of Cowan, 1985). These latter units are better understood and easily distinguished from the more controversial sediment-rich mélanges.

REGIONAL TECTONIC SETTING

An important point to stress is that the Pacific Rim Complex is actually a relatively small terrane. It lies along a major tectonic boundary that separates an older terrane assemblage from a more outboard assemblage formed during the Cenozoic. Thus, the present tectonic setting of the Pacific Rim Complex may be unrelated to the late Mesozoic setting in which it formed.

With respect to the Pacific Rim Complex, the geology of southwestern British Columbia and western Washington can be divided into four main tectonic elements (Fig. 2). The *continental framework* is an assemblage of Mesozoic and Paleozoic terranes that were added to western North America during a Late Cretaceous event (about 100 to 84 Ma), which involved the collision of Wrangellia and the formation of thrust nappes in the San Juan Islands and North Cascades (Monger and others, 1982; Brandon and others, 1988; Brandon, 1989b). Wrangellia is a large coherent terrane that underlies much of Vancouver Island and flanks the northeast side of the Pacific Rim Complex. The continental framework also includes the Coast Plutonic Complex of Canada, which is a suite of Late Cretaceous and younger plutons that intruded the older terranes (Monger and others, 1982). After collision, this tectonic assemblage formed a relatively coherent part of the North American continental mass, thus the term "continental framework."

Outboard of the continental framework lies a

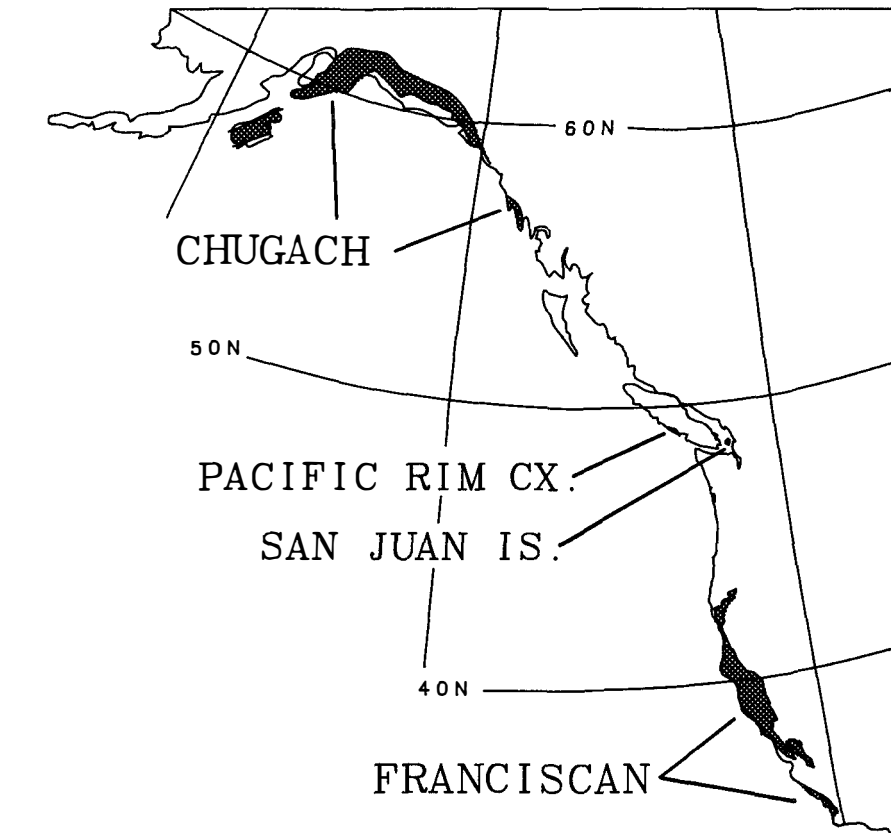


Figure 1. Upper Mesozoic mélangé units of western North America.

younger set of tectonic elements, which are bounded by faults of known or probable Cenozoic age (heavy-lined faults in Fig. 2). The first of these outboard elements, *displaced Mesozoic rocks* (Fig. 2), comprises several fault-bounded Mesozoic mélangé units: the Pacific Rim Complex, Pandora Peak unit, and Leech River schist (PRC, PP, and LRS in Fig. 2). These units presently lie along the western and southern perimeter of the continental framework. Previous interpretations considered these units to mark the trace of a late Mesozoic subduction zone (Dickinson, 1976; Muller, 1977a; Monger and others, 1982); however, almost all of the faults bounding these units are known to be Eocene in age (Leech River and San Juan faults: Fairchild and Cowan, 1982; Rusmore and Cowan, 1985; Tofino fault: Brandon, 1985; Clowes and others, 1987). The age of the Westcoast fault, which bounds the northeast side of the Pacific Rim Complex, is more poorly constrained. Indirect evidence (discussed below) suggests that it formed sometime during latest Cretaceous or early Tertiary time, which would be at least 45 m.y. after formation of the Pacific Rim mélanges. The interpretation that I prefer is that these fault-bounded slices represent displaced terranes rather than intact parts of a Jurassic-

Cretaceous subduction complex. They are geologically similar to some of the Late Cretaceous nappes in the San Juan Islands and may have been offset from there sometime during latest Cretaceous or early Tertiary time (Brandon, 1985).

The next of the outboard elements, *lower Eocene basalts*, lies outboard of the Pacific Rim Complex and other related displaced Mesozoic rocks. This regionally extensive terrane is composed of a thick (5 to 15 km), coherent sequence of basalt with a subordinate clastic cover. The basalts are commonly interpreted as an accreted seamount province that collided with the margin during Eocene time (for example, Wells and others, 1984). They are known as "Crescent Formation" in Washington (Tabor and Cady, 1978a) and "Metchosin Formation" on Vancouver Island (Muller, 1977a; Massey, 1986). Their extension into the offshore area (Fig. 2) is known from magnetic anomaly maps and drilling on the Vancouver Island shelf (Shouldice, 1971; MacLeod and others, 1977; Tiffin and Riddihough, 1977). Onland reflection profiles (Clowes and others, 1987) indicate that the Eocene basalts have been thrust a minimum of 25 km northeastward beneath Vancouver Island along the Leech River and Tofino faults. The

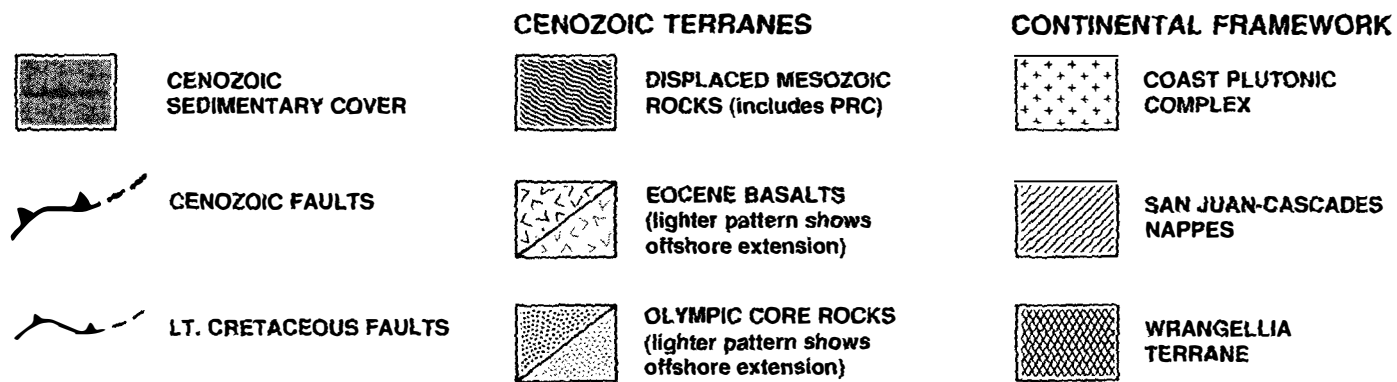
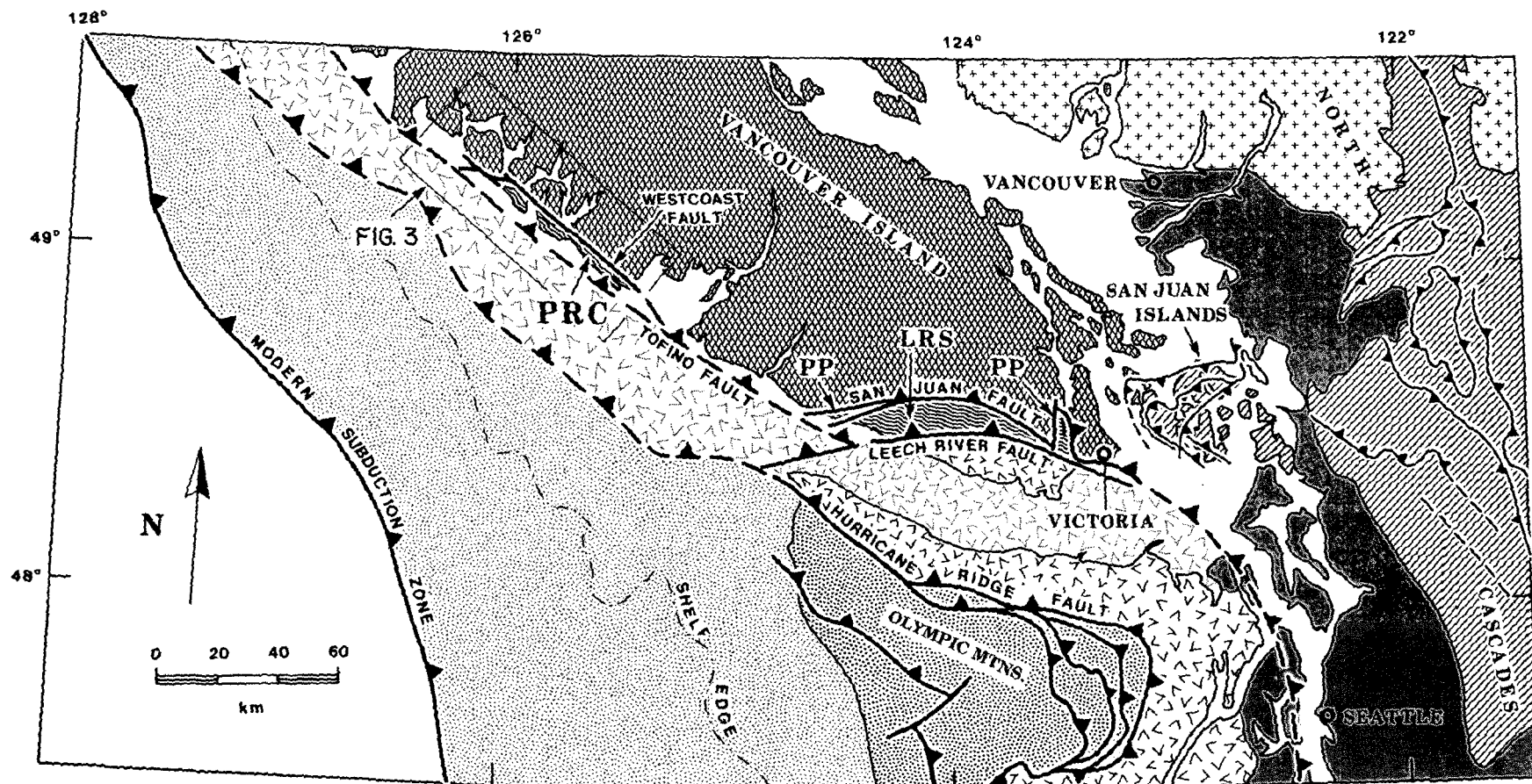


Figure 2. Tectonic map of the Vancouver Island area (after Clowes and others, 1987). The displaced Mesozoic rocks are abbreviated: PRC, Pacific Rim Complex; PP, Pandora Peak unit; and LRS, Leech River schist.

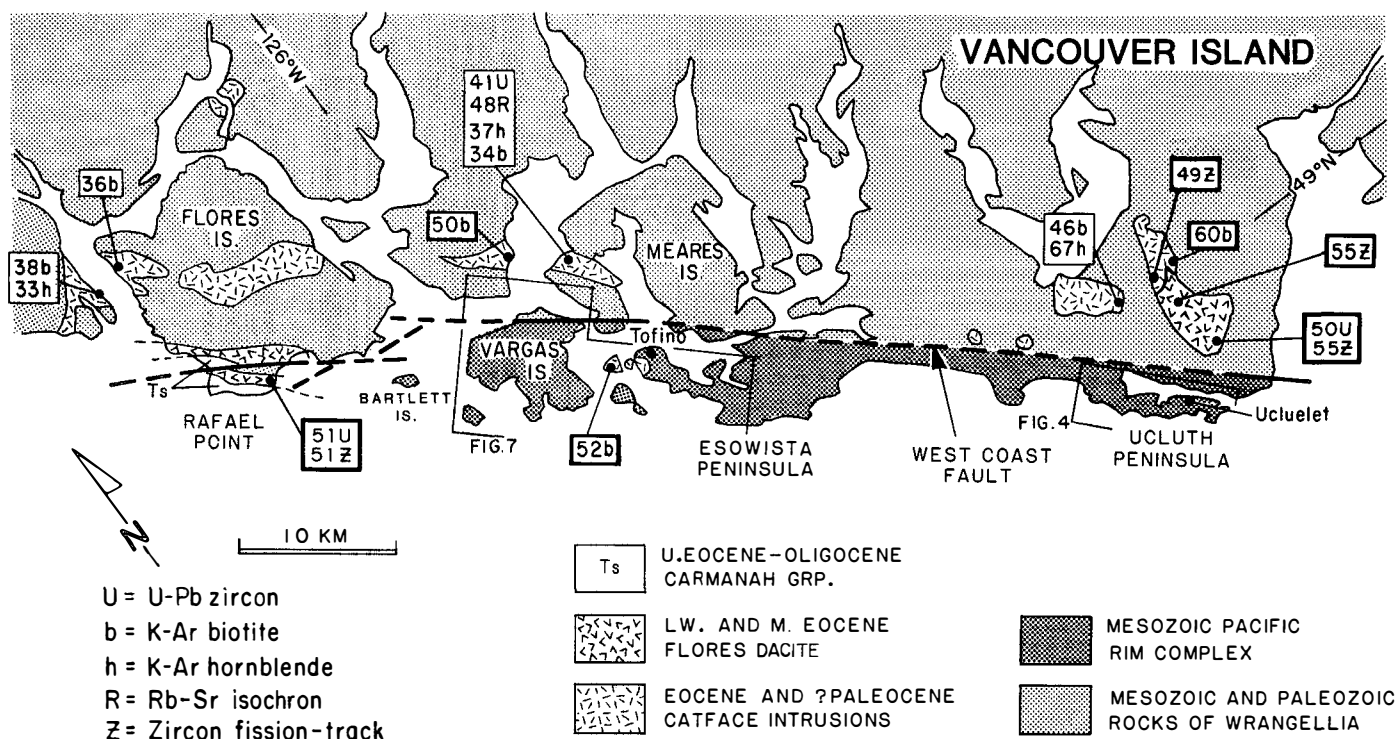


Figure 3. Geologic map of the Pacific Rim area, modified from Muller (1977b) to include my work. Outlined areas with figure numbers refer to the locations of detailed geologic maps. Isotopic ages are shown for lower Tertiary volcanic and plutonic rocks; ages outlined in heavy lines are from the older (50 m.y.) volcanic-plutonic suite discussed in the paper. All ages have been calculated using new decay constants (Harland and others, 1982). (Sources: K-Ar, Rb-Sr, and U-Pb ages for pluton on Meares Island: Isachsen, 1987; other K-Ar ages: Carson, 1973; Muller and others, 1981; zircon fission-track ages: J. A. Vance, 1983, 1986, written commun.; U-Pb ages for the Flores dacite: R. Parrish, 1986, written commun.)

Tofino fault is particularly important here, because it represents the western bounding fault for the Pacific Rim Complex.

The most outboard tectonic element, *Olympic Core rocks* (Tabor and Cady, 1978b), represents the modern Cenozoic subduction complex that formed west of the Eocene basalts, after their emplacement at the margin. The Olympic Core rocks underlie most of the offshore continental margin and are uplifted and exposed in the Olympic Mountains, northwest Washington State (Fig. 2). Reflection profiles across Vancouver Island demonstrate that this unit also extends some 50 km eastward beneath the island (Clowes and others, 1987).

OVERVIEW OF THE PACIFIC RIM COMPLEX

Evidence for Discrete Rock Units

On first impression, outcrops of the Pacific Rim Complex appear stratigraphically and structurally chaotic. One contributing factor is

the prevalence of high-angle faults, which commonly obscure the continuity of primary features. These faults are mostly Cenozoic in age because they commonly offset early Tertiary dikes and stratigraphic units. Fault separation is generally less than 100 m, but in some cases it does range to several kilometers. The dikes, which are ubiquitous in the Pacific Rim area, are related to local Eocene igneous activity (Catface Intrusions and Flores dacite in Fig. 3).

One area least affected by high-angle faulting is the seaward coast of the Ucluth Peninsula (Fig. 4), located at the southern end of the map area (Fig. 3). A broad anticline, trending obliquely (east-west) across the peninsula, exposes the two most complete sections through the Pacific Rim Complex. These sections reveal a coherent and relatively simple stratiform sequence, comprising three units: (1) the Ucluth Formation, a lower Mesozoic arc-volcanic unit; (2) unit 1, a Lower Cretaceous mudstone-rich mélangé; and (3) unit 2, an undated sandstone-rich mélangé. Figure 5 provides a summary description of these units; Table 1 and Figure 6

show available age data.¹ Mapping elsewhere in the Pacific Rim Complex indicates that these units are representative of the complex as a whole. Moreover, partial sections preserved in other locations are consistent with the stratigraphic succession found in the anticline. The following account relies heavily on relationships exposed in the anticline.

Ucluth Formation: Basement to the Mélangé Sequence

The Ucluth Formation (Brandon, 1989a) contains about 95% of all of the igneous rocks in the Pacific Rim Complex. The largest extent (≈4 km) of the unit is found in the Ucluth anticline (Fig. 4). Smaller exposures are present at the northern end of the map area (Fig. 7). The

¹All fossil localities and paleontologic results are catalogued in a separate appendix, available free of charge from the Geological Society of America Data Repository by requesting Supplementary Data 8916 from the GSA Documents Secretary.

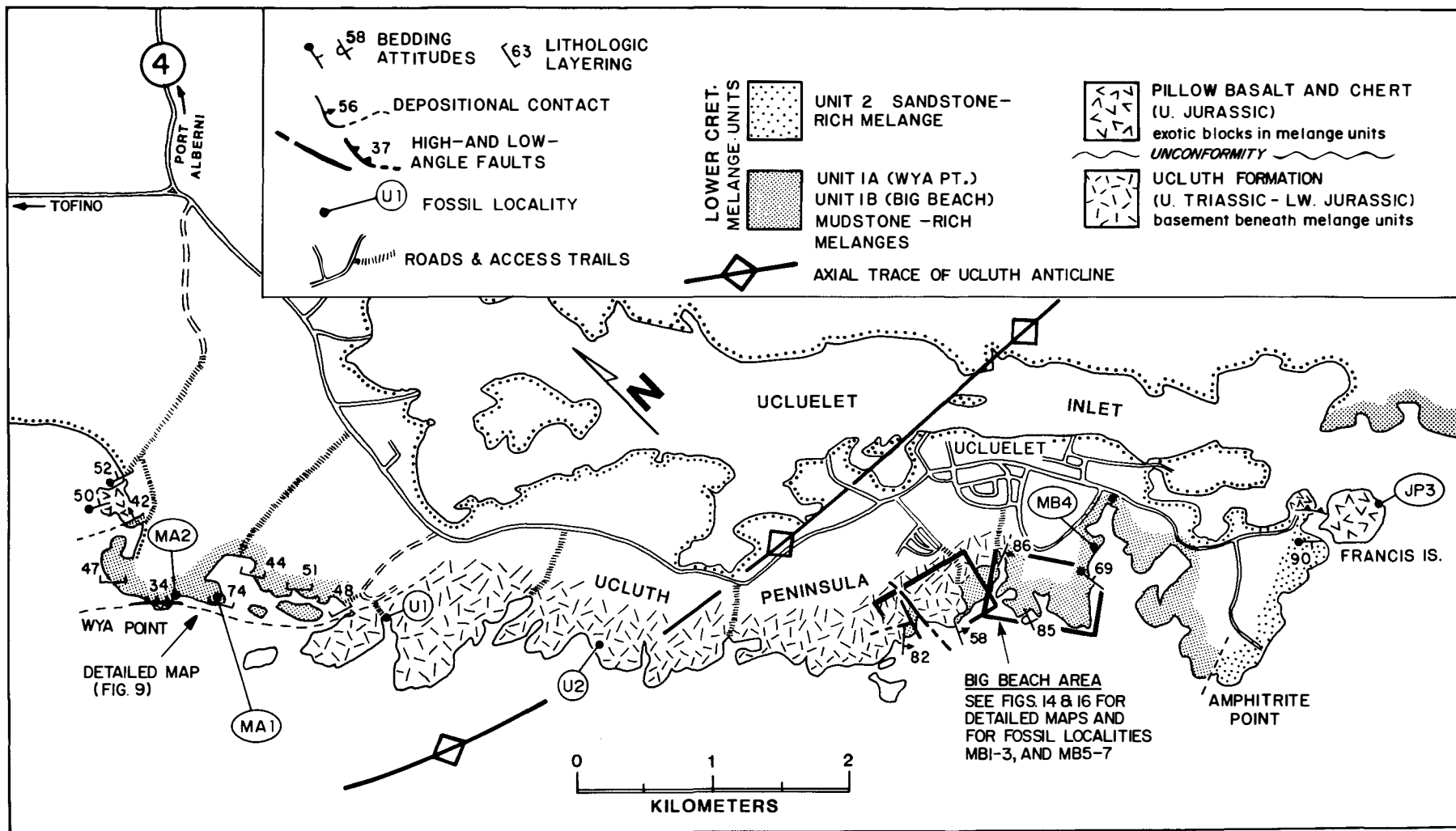
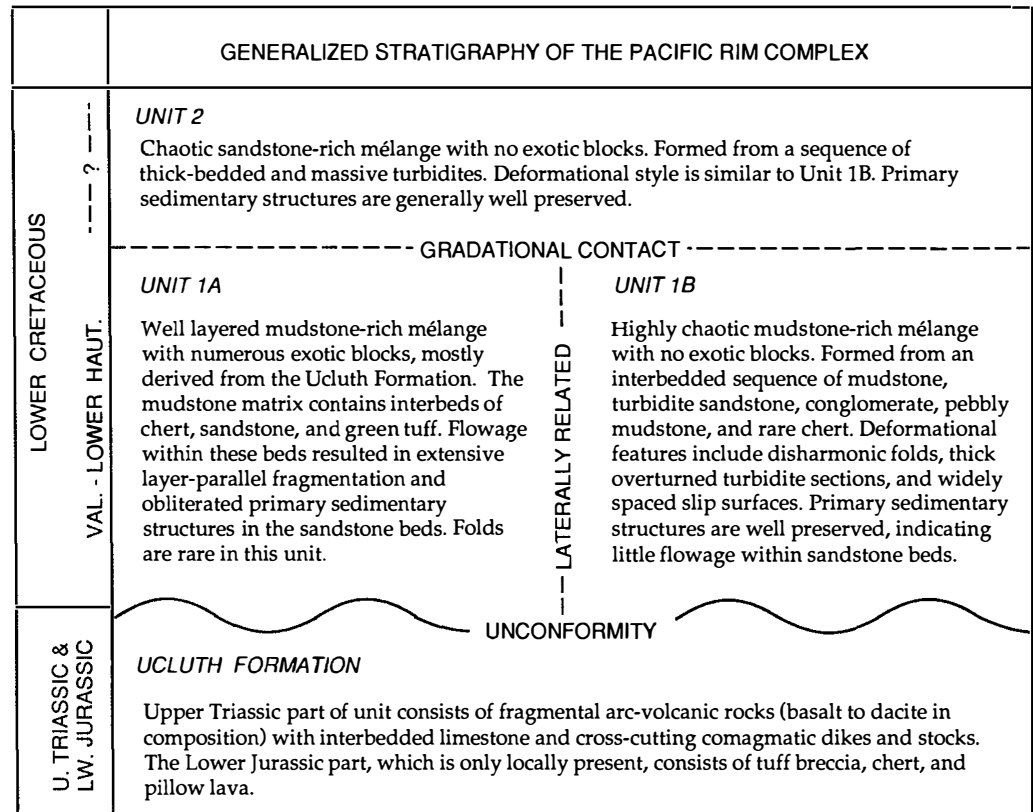


Figure 4. Geologic map of the Ucluth Peninsula, showing the relation between the Ucluth Formation and the overlying mélangé units. Heavy line indicates the approximate axial trace of the Ucluth anticline. See Figure 3 for location of map. Boxes show the location of maps in Figures 14 and 16.

Figure 5. Generalized stratigraphy of the Pacific Rim Complex.



Ucluth Formation consists mainly of fragmental volcanic rocks and is cut by numerous hypabyssal diorite intrusions. Fossils from interbeds of limestone and rare ribbon chert are Late Triassic and Early Jurassic, respectively (Table 1, Fig. 6). Major- and trace-element analyses indicate an arc-volcanic origin (moderate-potassium calc-alkaline series, $\text{SiO}_2 = 52\%$ to 65% , $\text{K}_2\text{O} = 0.8\%$ to 2.5% , $\text{TiO}_2 = 0.4\%$ to 1.6% ; Brandon, 1989a). The unit is further distinguished by widespread hydrothermal metamorphism, which resulted in the assemblage epidote + chlorite \pm calcite \pm white mica. This greenschist assemblage is found only in Ucluth rocks.

On the basis of their subduction-complex interpretation, Page (1974) and Muller (1977a) maintained that igneous rocks in the Pacific Rim Complex are fault slices derived from either subducting oceanic crust or the overriding Wrangellia terrane. Neither of these options is viable for the Ucluth Formation (Brandon, 1989a). The first option is precluded by the arc-volcanic character of the Ucluth. The second option is ruled out by fundamental differences in stratigraphy, age, and composition between the Ucluth Formation and the coeval units in Wrangellia (Karmutsen Basalts and the Quatsino Limestone; Fig. 6).

Units in the Mélange Sequence

The lowest mélange unit, unit 1, is distinguished mainly by the predominance of black mudstone. Otherwise, it is quite variable in lithology and deformational style. This variability is well illustrated in the Ucluth anticline, where unit 1 is divided into two subunits, 1A and 1B, exposed in opposite limbs of the anticline (Fig. 4). Unit 1A, which lies in the north limb, is characterized by a well-organized planar fabric, defined by interbedded mudstone, chert, sandstone, and green tuff. It contains numerous exotic blocks, most of which were derived from the Ucluth Formation. In contrast, unit 1B, exposed in the south limb, generally lacks exotic blocks and consists of a highly contorted assemblage of mudstone, turbidite sandstone, conglomerate, pebbly mudstone, and rare ribbon chert. Mapping elsewhere in the Pacific Rim Complex has shown that these two subunits represent end-member varieties of unit 1 and that all gradations between these end members are present. The matrix of unit 1 has yielded nine dated fossils (Table 1), which consistently indicate an Early Cretaceous age for the matrix sediments. The most precise ages are restricted to the interval Valanginian-early Hauterivian. A

locally preserved depositional contact at the base of unit 1B (described below) indicates that the unit 1 mélange stratigraphically overlies the Ucluth Formation.

Unit 2 gradationally overlies unit 1. It is composed almost entirely of massive and thick-bedded sandstone with minor mudstone and rare ribbon chert. Exotic blocks are absent. The style of deformation is much like that of unit 1B, consisting of a chaotic arrangement of bedding attitudes, many of which are overturned. This unit is undated but is inferred to be Early Cretaceous because of its gradational relationship with unit 1.

According to the classification scheme of Cowan (1985), unit 1A would correspond to his Type II and Type III mélanges, and units 1B and 2 to his Type I mélange.

Regional Prehnite-Lawsonite Metamorphism

All of the Pacific Rim Complex has experienced a very low-temperature, high-pressure metamorphism, marked by the characteristic assemblage prehnite \pm lawsonite + calcite. This assemblage is ubiquitous, but it rarely constitutes more than 3% to 5% of the rock. It is found in veins and also as a replacement of plagioclase.

Because metamorphism mainly involved phase changes among Ca-Al-Si minerals, this assemblage is best developed in sandstones of the mélangé units, which are rich in andesitic volcanic detritus. These sandstones typically contain prehnite ± lawsonite + calcite ± white mica ± chlorite as coexisting metamorphic phases in contact with detrital plagioclase and quartz. In some cases, a more restricted assemblage, calcite + white mica, was formed, probably owing to CO₂ in the fluid phase (Thompson, 1971). Metamorphism postdates the Early Cretaceous age of the mélanges (130 m.y.) and predates the lower Eocene plutons and dikes that intruded the Pacific Rim Complex (~50 m.y. ago). Peak metamorphic conditions are estimated at about 150 °C and in excess of 3.5 kb (350 MPa) (compare with Brandon and others, 1988).

Coexisting prehnite and lawsonite represent a very unusual metamorphic assemblage, which appears to be unique to the Late Cretaceous nappes of the San Juan Islands and North Cascades. Notable exceptions are the Pacific Rim Complex and the related Pandora Peak unit. Metamorphism of the San Juan-Cascades nappes occurred during the collision of Wrangellia at 100 to 84 Ma (Brandon and others, 1988). It is argued below that the Pacific Rim Complex may have formed part of this nappe sequence. If this is correct, then metamorphism would have postdated formation of the Pacific Rim mélanges by at least 30 m.y.

UNIT 1A: MUDSTONE-CHERT MÉLANGE WITH EXOTIC BLOCKS

The type locality for unit 1A is Wya Point, located on the northwest side of the Ucluth Peninsula (Fig. 4). In this area, the unit is more than 600 m thick. Layering within the mélangé dips consistently to the north, at about 40° to 60°. An unfortunate aspect of the Wya Point exposures is that the contact of unit 1A with the Ucluth Formation is only locally exposed in a 50-m-long segment of coastline. Much of that contact consists of a moderately dipping fault that strikes obliquely across the contact and continues upward into unit 1A. The remaining segments of the contact are remnants of an unfaulted primary contact between unit 1A and the Ucluth Formation, but these segments are too short to interpret with much confidence.

Internally, unit 1A is a typical blocks-in-matrix mélangé. The matrix consists of an inter-layered sequence of black mudstone (55%), ribbon chert (25%), sandstone (15%), and green tuff (5%) (percentages indicate relative proportions). Exotic blocks are ubiquitous but actually constitute a relatively small proportion of the total unit (<5%–10%).

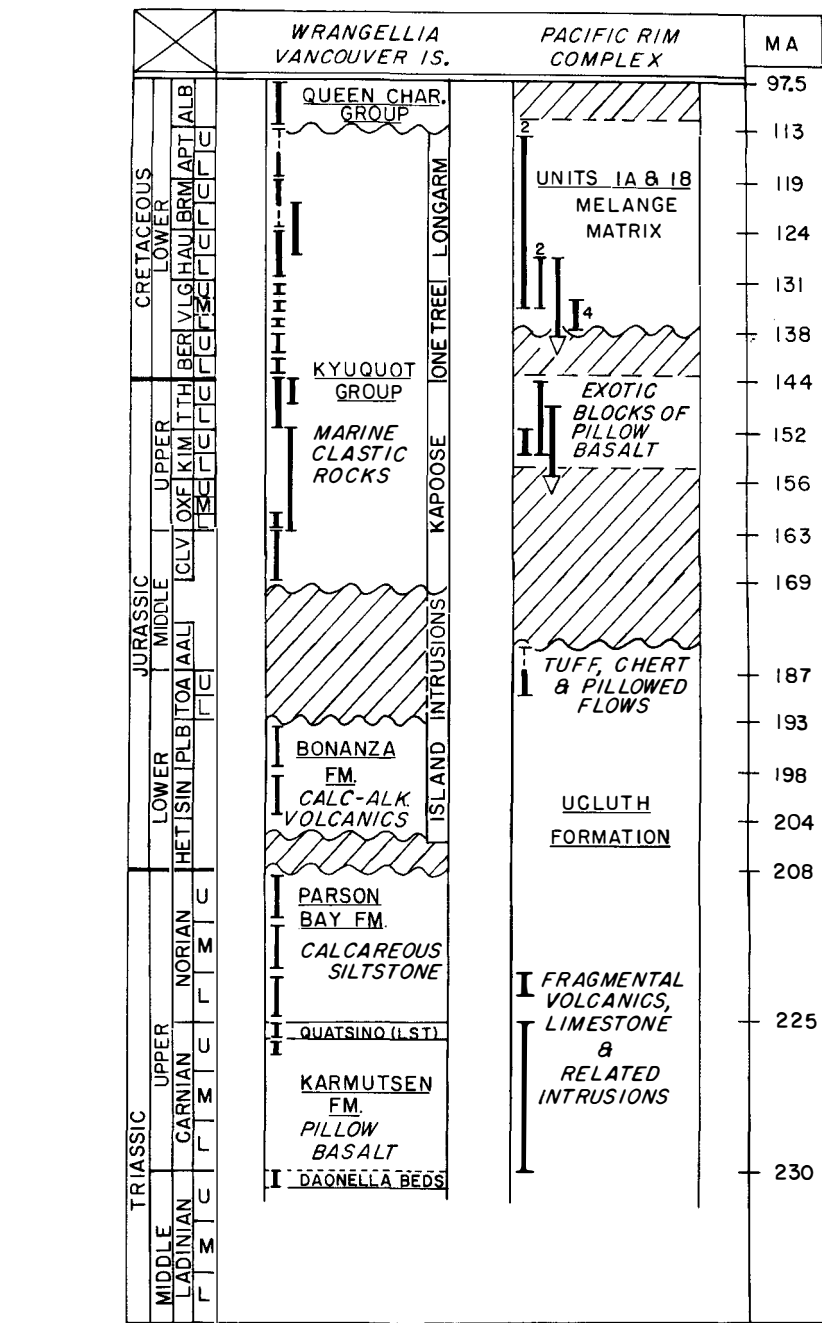


Figure 6. Stratigraphic comparison of the Pacific Rim Complex with Mesozoic units of the Wrangellia terrane, Vancouver Island. Fossil ages are indicated by a bracketed line, which shows the precision of the age determination. For the Pacific Rim Complex, a number is shown if there is more than one locality of that age. Fossil ages for Wrangellia units are summarized from Muller and others (1974, 1981) and other sources cited therein, and those for the Pacific Rim Complex are from Table 1. The absolute time scale shown on the right is from Kent and Gradstein (1985).

Structure and Fabric of Matrix

A striking feature of unit 1A is its well-layered but highly disrupted fabric. On a local scale (<2 m), this fabric is dominated by oblate-

and spheroidal-shaped fragments of chert and sandstone (Figs. 8 and 9), which range considerably in size and aspect ratio. Most of these fragments were formed by disruption of thin isolated beds of ribbon chert and sandstone. In some

TABLE 1. FOSSILS FROM THE PACIFIC RIM COMPLEX

No.	Geologic setting and location	Fossils	Age
<i>Ucluth Formation</i>			
U1	Limestone interbedded with volcanic breccia. Ucluth Peninsula (Fig. 4)	Conodonts	Late Triassic, late Early Norian
U2	Limestone interbedded with volcanic rocks and intruded by diorite dike. Ucluth Peninsula (Fig. 4)	(a) conodonts (b) ammonoids	Late Triassic, Carnian Probably Late Triassic
U3	Ribbon chert interbedded with pillow lava and tuff, tentatively assigned to the Ucluth Formation. Vargas Is. (Fig. 7)	Radiolaria	Early Jurassic, middle or late Toarcian (or possibly earliest M. Jurassic)
<i>Upper Jurassic pillow basalt blocks in unit 1 mélange</i>			
JP1	Red ribbon chert from block in mélange. 5 km SE of Ucluelet	Radiolaria	Late Jurassic, late Kimmeridgian
JP2	Ribbon chert interbedded with pillow basalt (ocean-floor-type basalt). SE side of Ucluelet Inlet	Radiolaria	Late Jurassic, late Kimmeridgian to late Tithonian
JP3	Ribbon chert interbedded with pillow basalt (ocean-floor-type basalt). Francis Is., SE of Ucluelet (Fig. 4)	Radiolaria	Middle or Late Jurassic, Aalenian to early Tithonian
<i>Fossils from the matrix of unit 1A mélange</i>			
MA1	30-cm-thick lens of ribbon chert, interbedded with mudstone matrix. Wya Pt., Ucluth Peninsula (Figs. 4 and 9)	Radiolaria	Early Cretaceous, Late Valanginian to late Aptian
MA2	75-cm-thick lens of ribbon chert, interbedded with mudstone matrix. Wya Pt., Ucluth Peninsula (Fig. 4)	Radiolaria	Early Cretaceous, probably Late Valanginian or Hauterivian
MA3	Poorly exposed chert sequence in mudstone matrix of mélange. Blunden Is., W of Vargas Is. (Fig. 7)	Radiolaria	Early Cretaceous, Late Valanginian to late Aptian
<i>Fossils from the matrix of unit 1B mélange</i>			
MB1	Chert interbedded in mudstone and turbidite sequence. S of Big Beach (Fig. 14)	Radiolaria	Early Cretaceous, Late Valanginian or early Hauterivian
MB2	Chert interbedded in turbidite sequence. S of Big Beach (Fig. 14)	Radiolaria	Late Jurassic to Early Cretaceous, late Tithonian to early Hauterivian
MB3	Coquina bed in laminated black mudstone. Big Beach area (Fig. 14)	<i>Buchia pacifica</i>	Early Cretaceous, middle Valanginian
MB4	Coquina bed in laminated black mudstone. S of Big Beach (Fig. 4)	<i>Buchia pacifica</i>	Early Cretaceous, middle Valanginian
MB5	Coquina bed in laminated black mudstone. N of Big Beach (Fig. 16)	<i>Buchia pacifica</i> and <i>B. tolmatschowi</i>	Early Cretaceous, early or middle Valanginian
MB6	Massive black mudstone at base of unit 1B; unconformably overlies Ucluth Formation. N of Big Beach (Fig. 16)	<i>Buchia pacifica</i> and <i>B. tolmatschowi</i>	Early Cretaceous, early or middle Valanginian
MB7	Laminated black mudstone and turbidite sandstone. Big Beach area (Fig. 14).	<i>Inoceramus?</i>	Age not known

Note: appendix contains paleontological reports and detailed descriptions of the geologic setting for the above fossil localities. Localities JPI, MB3, and MB4 were originally reported in Muller and others (1981); JP2 and JP3 are from unpublished data of J. E. Muller and E. A. Pessagno, Jr. The remaining localities were collected by Brandon. Chemical analyses for pillow basalts at JP2 and JP3 are reported in Brandon (1989a).

respects, they resemble boudins, but instead of the "sausage-like" shapes typical of boudinage (Ramsay, 1967), the fragments are pancake shaped, suggesting axial-symmetric layer-parallel extension (compare with Cowan, 1982a). An unusual feature is that the amount of separation between fragments tends to increase as the fragments become more spheroidal, suggesting that fragmentation may have been produced, at least in part, by internal flowage and thickening of the fragments, as opposed to bulk layer-parallel extension. The more oblate fragments are well aligned, producing a strong planar fabric ("fragment foliation" of Cowan, 1985). This fabric lacks any obvious evidence of systematically rotated fragments or asymmetric fragment

shapes, indicating that the strain path during mélange deformation was generally coaxial and cannot be attributed to simple shearing.

The layered appearance of the mélange is accentuated by thicker lenses of sandstone and chert (> 1 m) that parallel the fragment foliation. An observation with important mechanical implications is that these thick lenses tend to be less deformed and more laterally persistent than do their more thinly bedded counterparts (Figs. 8a and 8b). In areas without thick lenses, the mélange still maintains a layered appearance, defined by changes, on the scale of 1 to 2 m, in the relative proportions of chert and sandstone in the mudstone.

The mélange fabric maintains a consistently

planar orientation at both map and outcrop scale (Fig. 10a). Outcrop-scale folds are rare. At Wya Point, this layered fabric dips moderately to the northeast and parallels the contact of unit 1A with the underlying Ucluth Formation (Fig. 4).

The coarser-grained sediments in the matrix of this mélange (sandstone, green tuff, and chert) show evidence of extensive internal flowage. In this regard, the most important observation is the complete lack of primary sedimentary structures in sandstones of unit 1A. Furthermore, many of the original beds of sandstone, chert, and green tuff have been distorted into irregular shapes, some lenticular and some podiform (Figs. 8 and 9). Small clastic dikes are also present, but are rare (Fig. 8c). Thin-section observations indicate that this deformation was accommodated by ductile particulate flow (Borradaile, 1981) while the sediments were still loose granular aggregates. Sandstones show some brittle deformation, such as grain breakage and small faults with millimeter-scale offsets (web structure of Byrne, 1984), but these features are relatively insignificant and account for only a minor amount of the total strain.

It is interesting to note that beds of chert and sand appear to have deformed in a similar fashion during formation of the mélange. Initially, these chert beds were probably composed of fine-grained radiolarian sand, deposited by turbidity and contour currents (Jenkyns and Winterer, 1982). Thus, if the chert was deformed prior to consolidation, then it would probably have responded like a loose sandy aggregate.

In contrast to the coarser sediments, the mudstone fraction of the matrix appears relatively undeformed. It lacks such features as a pervasive scaly cleavage, slickensided fault surfaces, or a streaky "shear" foliation. Locally, the mudstone does contain a sporadic spaced cleavage, oriented parallel to the mélange layering. In thin section, the cleavage folia are marked by a concentration of opaque (insoluble) minerals, a feature distinctive of solution mass transfer (Borradaile and others, 1982). Cleavage formation is attributed to late-stage pressure solution, after formation and lithification of the mélange. The degree of cleavage development bears no systematic relation to the degree of disruption in the mélange.

In studies of many other mudstone-rich mélanges, the mudstone matrix is inferred to have accommodated large shear strains, whereas in this mélange, the coarser-grained fraction of the matrix bears the most obvious signs of deformation. There is no evidence that large shear strains were localized in the mudstone or that it behaved with the same mobility as the sandstone, chert, and green tuff.

Age of Matrix Sediments

The age of unit 1A is based on radiolaria from ribbon chert interbedded in the *mélange* matrix. This relationship may seem unusual because chert is commonly considered an exotic component of a *mélange*. In this case, however, chert is indigenous, constituting about 25% of the matrix. It was deposited in isolated ribbon beds, now highly fragmented, and also in thin coherent lenses averaging about 0.5×10 m in size and containing from 5 to 20 ribbon beds. Bedding features and radiolaria are relatively well preserved in the lenses, whereas the isolated beds tend to be more recrystallized and typically lack visible radiolaria. Chert-mudstone contacts generally show no signs of localized shear and faulting and thus are considered to be depositional. Further evidence of a depositional relationship is the common presence of thin sandy interbeds in the chert lenses, including one of the dated lenses (MA1 in Table 1). Thin sections reveal that the chert itself contains variable amounts of mud- and sand-sized clastic material, similar to the mudstone and sandstone in the surrounding matrix. Jones and Murchey (1986) described similar relations for their chert-mudstone lithofacies association, which they attributed to deposition in a continental-margin setting.

Composition and Source of Exotic Blocks

Blocks in unit 1A are generally monolithic and consist of either igneous rock or limestone. They are clearly extraformational with respect to the matrix sediments and can be divided into two groups. Most blocks (>80%) belong to the first group, which consists mainly of diorite with minor limestone and fragmental volcanic rock, all of which were derived from the Ucluth Formation. The diorite blocks locally contain screens of fragmental volcanic rock, indicating that the diorite was originally intruded into a volcanic country rock. In thin section, the diorite blocks consist of medium-grained plagioclase and quartz, plus minor hornblende and biotite. Both the diorite and volcanic blocks are variably altered to chlorite-epidote assemblages and are cut by numerous small faults and cataclastic shear zones. These brittle structures postdate chlorite-epidote alteration and predate the formation of rare prehnite-lawsonite-calcite veins, related to regional high-pressure metamorphism.

The second, and more subordinate, group has no local source terrain. It comprises blocks of Upper Jurassic pillow basalt and rare ultramafite (serpentinized clinopyroxenite). Mapping of the Pacific Rim Complex has identified about

20 pillow basalt blocks and only 2 ultramafite blocks, all of which are confined to the unit 1 *mélange*. The ultramafite blocks are restricted to a single location on southern Vargas Island (Fig. 7), where they are bounded and cut by several brittle-style faults. In contrast, the pillow basalt blocks are widely distributed. They generally show little internal deformation. Radiolaria from interbedded ribbon cherts indicate a Late, and possibly Middle, Jurassic age for the pillow basalts (Table 1). Major- and trace-element analyses indicate an ocean-floor origin for the basalts (Brandon, 1989a; low-potassium tholeiites, $\text{SiO}_2 = 50\%$ to 55% , $\text{TiO}_2 = 1.2\%$ to 2.7% , $\text{K}_2\text{O} = 0.1\%$ to 0.4%), at either a mid-ocean ridge or a back-arc rift. The basalts are clearly different from the Ucluth Formation.

Block-Matrix Relationships

The size of the exotic blocks varies considerably, with dimensions ranging from less than a meter to more than 250 m. As shown in Table 2, limestone and fragmental volcanic rock are restricted to relatively small blocks, whereas pillow basalt and ultramafite occur only as large blocks. The more numerous diorite blocks span the whole range. Most blocks, especially the larger ones, are slab shaped, with average aspect

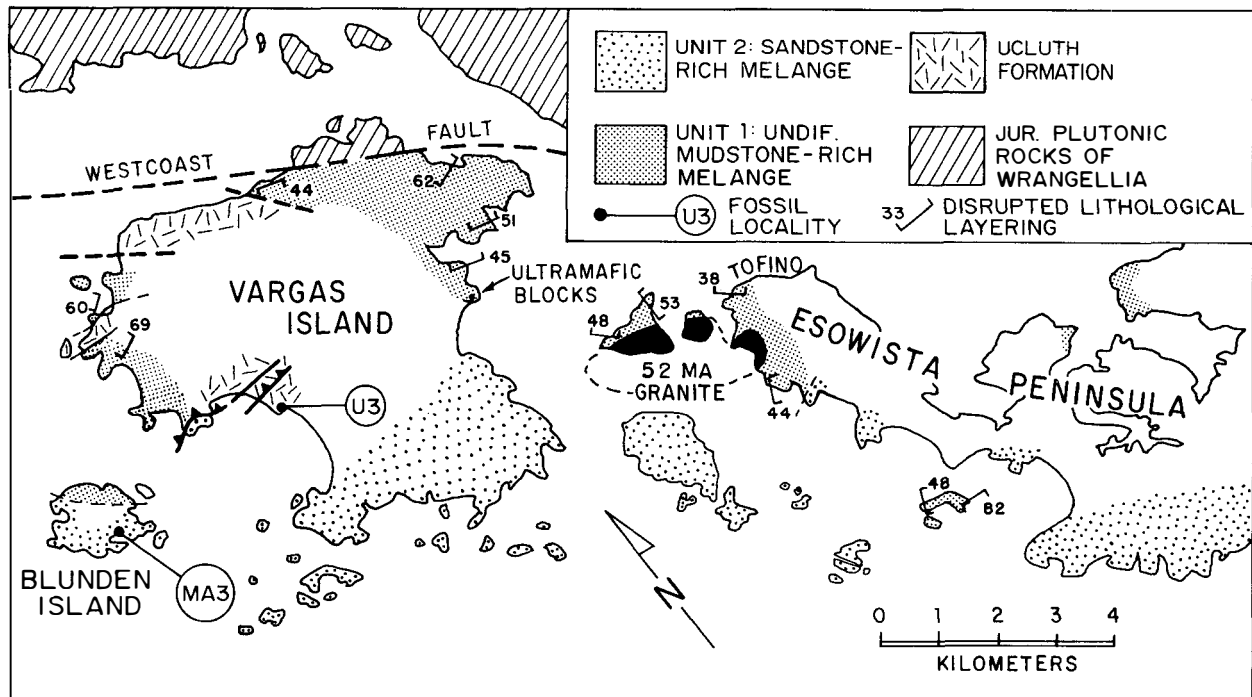


Figure 7. Geologic map of the Esowista Peninsula-Vargas Island area, located at the northwest end of the Pacific Rim area. See Figure 3 for location. Fossil locality MA3 is from an isolated exposure of unit 1 *mélange*.

TABLE 2. DIMENSIONS OF BLOCKS IN UNIT 1A

Block type	Average size (thickness × length)	Average aspect ratio	Maximum size (thickness × length)
Diorite	3 × 14 m	5	6 × 45 m (Wya Pt.) 190 × ? m (Vargas Is.)
Limestone and fragmental andesite	1 × 1.5 m	1.5	~2 × 2 m (Wya Pt.)
Pillow basalt	100 × >150 m	..	>220 × >300 m (Wya Pt.)
Ultramafite	8 × 70 m	9	10 × 100 m (Vargas Is.)

ratios (length/thickness) of about 6. An important observation is that the tabular shapes of the blocks are everywhere strongly aligned with the mélange fabric, which tends to accentuate the layered appearance of the mélange even further.

The matrix sediments adjacent to the blocks might be expected to show evidence of brittle or ductile shear, such as slickensided faults, fault-zone fragmentation, scaly cleavage, streaky “shear” foliation, folded layers, or rotated clasts. Locally, some of these features are present. For instance, the ultramafite blocks are bounded and cut by several brittle-style faults. In another case, matrix sediments beneath the pillow basalt block at Wya Point contain a few thin ductile shear zones. The critical observation, however, is that the overwhelming majority of blocks lack evidence of brittle or ductile shear in the adjacent matrix sediments. For instance, Figure 11 shows a cross-sectional view of a large diorite block (4.5 by >35 m in map view). The degree of disruption in the surrounding matrix does not change systematically with distance from the block contacts. Instead, the mélange fabric parallels the irregular contours of the block. The large diorite block in Figure 9 (6 by 45 m in map view) shows a similar relationship. Furthermore, the upper contact of the block is mantled by a thin lens of well-bedded ribbon chert, which has yielded Early Cretaceous radiolaria (MA1 in Table 1). These observations preclude introduction of the blocks into the mélange by deep-seated tectonic processes, such as imbricate faulting at a subduction-zone thrust, or plucking and transport by a ductilely flowing matrix (for example, flow mélange of Cloos, 1984).

Significance of Green Tuff

Green tuff forms a minor but enigmatic part of the mélange matrix. It is found as small (<1 m) irregular bodies, which in the field appear to be composed of fine-grained volcanic material. Thin sections reveal that this rock is not pyro-

clastic but instead is composed of poorly sorted clasts of metavolcanic and metaplutonic rocks (Brandon, 1989a). The term “green tuff” is therefore a misnomer, but I continue to use it herein because it has become a common field term used to describe similar green sedimentary rocks in other mudstone-rich mélanges (for example, Cowan, 1985).

Three types of green tuff have been recognized, each distinguished by a unique source rock: (1) microcrystalline basalt altered to chlorite; (2) plagiophyric andesite with plagioclase partially altered to chlorite; and (3) medium-grained diorite with minor epidote. Chlorite and epidote alteration assemblages formed in the source rocks prior to deposition of the tuff, as indicated by monomineralic clasts of epidote and by lithic clasts with boundaries that truncate alteration assemblages. Chemical analyses indicate that some tuff samples are compositionally similar to Ucluth volcanic rocks, whereas others match the Jurassic pillow basalts (Brandon, 1989a). Thus, this sediment is interpreted to be a scree deposit derived from exotic blocks in the mélange and perhaps from nearby scarps of Ucluth Formation and Jurassic basalts. The sediment may have been locally reworked by bottom currents and ponded in small depressions, which would explain why some tuff bodies are separated by distances of more than 5 to 10 m from the nearest exotic block or tuff body.

Interpretation of Unit 1A

I consider the matrix of unit 1A to have originated as a Lower Cretaceous sequence of interbedded mud, chert, sand, and green tuff. Formation of the mélange involved extensive disruption and fragmentation of bedding, but the original stratified nature of this sequence was not destroyed and is probably largely responsible for the layered appearance of the mélange.

One of the most striking features of unit 1A—pervasive layer-parallel fragmentation—is attributed to lateral flowage of coarse sediments within individual beds. Layer-parallel fragmentation has been recognized in many other sediment-rich mélanges (Cowan, 1985) and is commonly interpreted as axial-symmetric (“chocolate-tablet”) boudinage of competent layers due to large extensional strains in all directions within the plane of layering (Fig. 12a; Cowan, 1982a; Byrne, 1984). The interpretation proposed here represents a nonextensional form of boudinage (Fig. 12b), whereby internal flowage causes a highly incompetent bed to separate and thicken into boudin-like shapes in the absence of bulk extensional strain. This conclusion is based on the following observations.

(1) Spheroidal fragments tend to be more widely separated than are ellipsoidal fragments, which implies that the amount of separation is controlled by layer-perpendicular thickening within the fragments. Evidence of this thickening is illustrated by the bulbous protrusions found on the upper and lower sides of some sandstone fragments (Fig. 8d; also Cowan, 1982a).

(2) Fragmentation of sand and chert beds by layer-parallel extension would require an equal or larger amount of extensional strain in the surrounding mud, and yet the mudstone shows no evidence that it accommodated large strains during formation of the mélange. It seems unlikely that the mud could have experienced large strains without the formation of a visible fabric, such as a strong preferred orientation of phyllosilicate grains (Oertel, 1983).

(3) Field observations (Ramsay, 1967) and theoretical analysis (for example, Smith, 1977) of true boudinage show that within a given layer, the necking instability produces boudins with a highly periodic shape, size, and spacing. This is in marked contrast to the irregular shape, size, and spacing of fragments in unit 1A (Figs. 8 and 9).

(4) The amount of separation between fragments varies widely from layer to layer. If fragmentation were due to layer-parallel extension, then the strain field would have to fluctuate widely at a wavelength of 10 to 20 cm in a direction perpendicular to the mélange layering. This type of variability might be possible in a ductile shear zone, but the mélange shows no obvious evidence of noncoaxial shear or zones of strain localization.

Although these observations do not prove a nonextensional origin for layer-parallel fragmentation in unit 1A, they do argue strongly against conventional boudinage. Overall, deformation seems to have preferentially affected the coarser fraction of the matrix sediments (sand, tuff, and radiolarian sand), resulting in fragmentation of thin-bedded sediments, extensive flowage within thicker beds, and obliteration of primary sedimentary structures.

An alternative interpretation considered herein is that deformation was caused by seismically induced liquefaction. Research in soil mechanics (reviewed below) has shown that this phenomenon tends to preferentially affect poorly drained, coarse sediments, such as sands and silts. Liquefaction may have permitted the sand, tuff, and radiolarian sand to have flowed laterally, resulting in fragmented beds with only minor deformation of the adjacent mud.

The origin of the exotic blocks, that is, the process responsible for their transport and em-

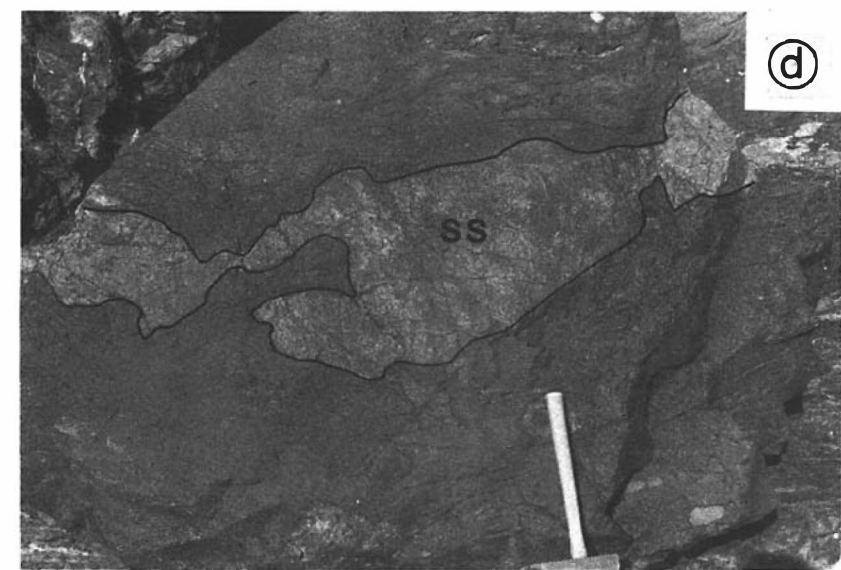
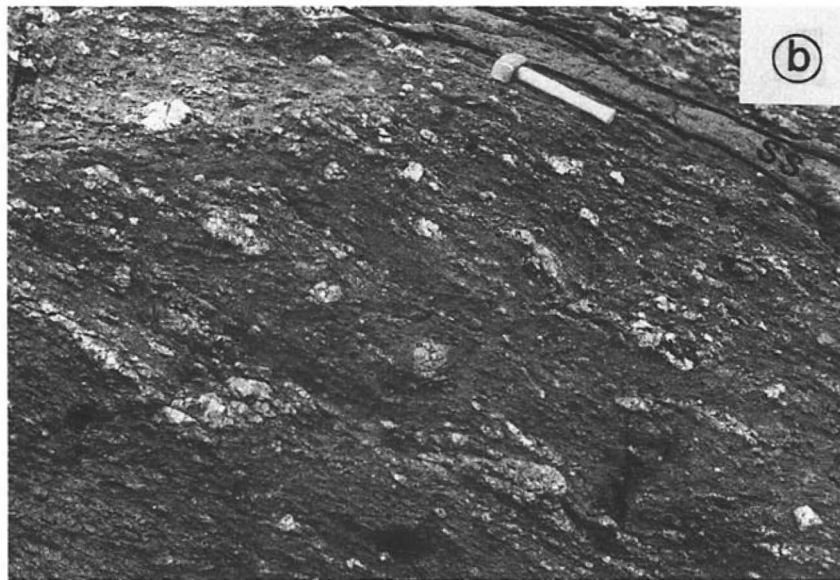


Figure 8. Photographs of structures in unit 1A mélangé. (a) A typical example of the planar fabric of the mélangé, defined by tabular layers of sandstone (ss) and ribbon chert (ch), and also by aligned fragments of chert and sandstone. The surrounding darker rock is black mudstone. The stratigraphic base of the mélangé is to the left (southwest). (b) Close-up of the upper right corner of a. Note that the rock hammer is in the same position in both photographs. The ellipsoidal and spheroidal fragments are mostly chert.

Figure 8. (Continued) (c and d) Some examples of podiform sandstone bodies commonly found in this mélangé. The tail-like feature emanating from the sandstone pod in c may represent a miniature sandstone dike that intruded the surrounding mudstone. For scale, a knife and a hammer are shown in c and d, respectively.

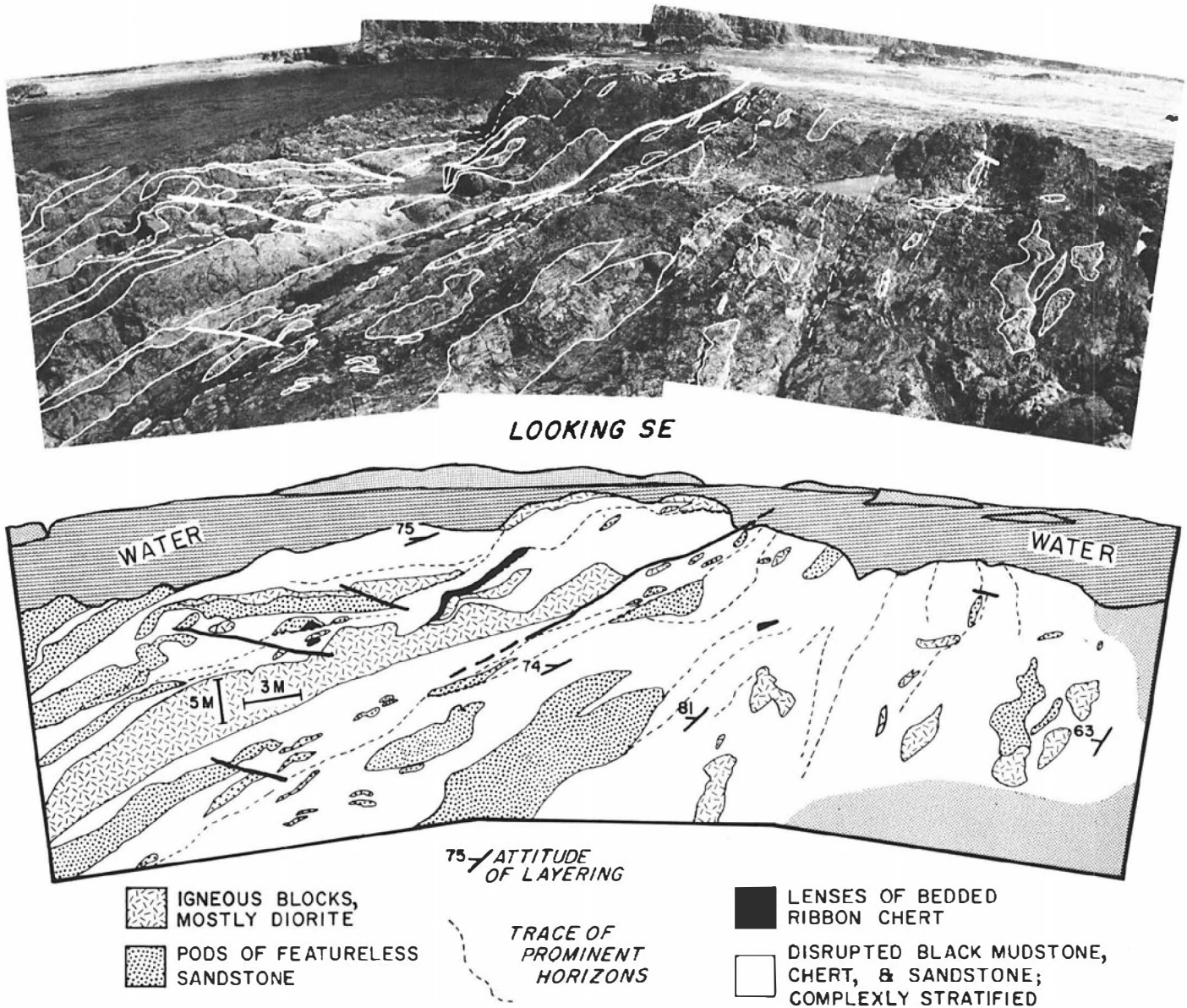


Figure 9. Outcrop map of mélangé fabric in unit 1A (location shown in Fig. 4). The map was prepared from an oblique photograph (upper half of figure) and is oriented facing to the southeast. Note that contacts are distorted by perspective and also by small topographic irregularities, especially in the upper central part of the map, which contains a prominent high. The large diorite block shown on the left side of the map is 45 m long and 6 m wide. The top of this block is mantled by a lens of radiolarian ribbon chert (black layer in center of map) that has yielded Early Cretaceous radiolaria (MA1 in Table 1). The base of unit 1A lies about 50 m off the right (southwest) side of the map.

placement into the matrix, appears unrelated to the deformation of the matrix sediments. The preservation of a stratified mélangé matrix and the absence of a pronounced deformational fabric in the mudstone preclude an origin by imbricate faulting, deep-seated flow mélanges, or surficial debris flows.

I suggest that the blocks represent submarine rock falls derived from basement highs that exposed the Ucluth Formation and another, more cryptic terrane composed of Upper Jurassic ophiolitic rocks. This interpretation is compati-

ble with the large size and angular, elongate shapes of the blocks and with the presence of plutonic and volcanic scree (green tuff) in the matrix sediments. The basement highs may have been bounded by fault scarps, which might account for the sporadic cataclastic deformation found in the diorite blocks. The matrix sediments would represent a basinal sequence deposited near these scarps. I infer that the blocks slid for some distance over the soft, muddy surface of this basin before they came to rest. Prior and others (1984) described an analogous situa-

tion in a modern submarine landslide where large slab-like blocks, which they called "out-runner blocks," separated from the front of the slide and glided across the sea floor for distances of as much as 300 m. Naylor (1982) and Ineson (1985) have documented two ancient examples. They both noted that sediments at the margins of these blocks commonly lack evidence of emplacement-related shearing. High fluid pressures may be responsible for decoupling the moving block from the underlying sediments.

What keeps a block from sinking into the

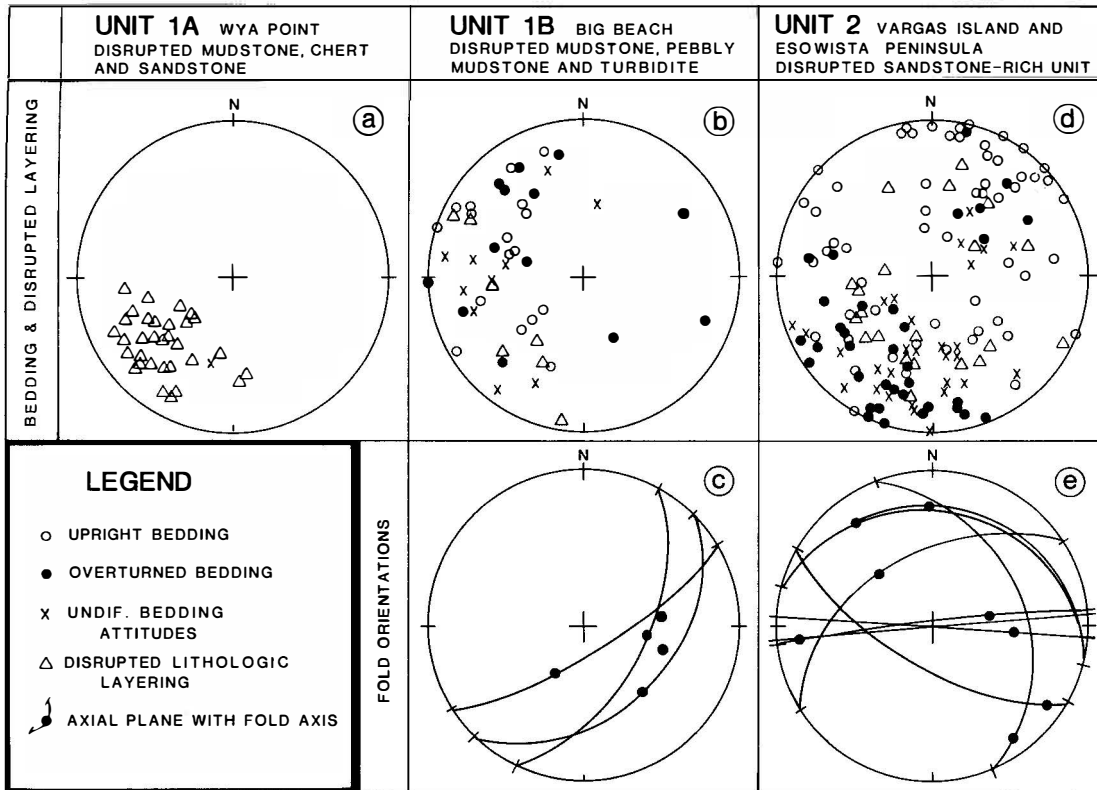


Figure 10. Stereograms of structural features in the mélangé units (equal-area, lower-hemisphere projection). These plots illustrate the difference between the planar fabric of unit 1A and the chaotic and folded fabric of units 1B and 2. The axes and axial planes shown in c and e are from small outcrop-scale folds (see text).

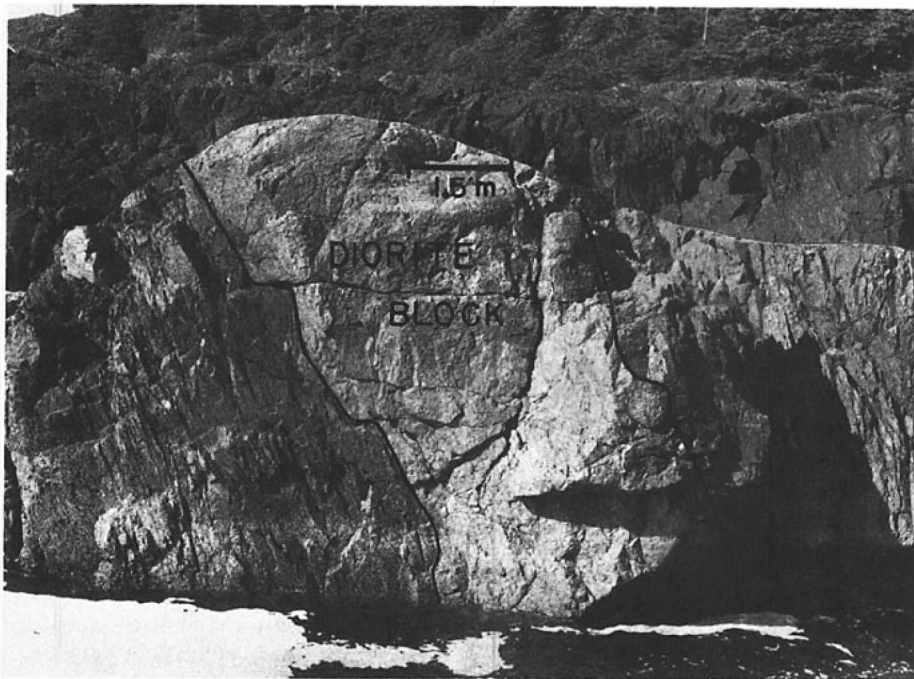


Figure 11. Photograph of a large diorite block in unit 1A mélangé (looking northwest). The block is about 4.5 m thick and extends for more than 35 m along strike. The block preserves primary contact relations with no evidence of shearing or brittle faulting. The base of the mélangé is to the left (southwest).

surface sediments after it comes to rest? Naylor (1982) has analyzed this problem, utilizing foundation-engineering methods to determine the static load limits for undrained failure beneath various-shaped blocks. His analysis (Fig. 13) illustrates the conditions necessary for a block to remain statically supported at the surface. It predicts that average- and maximum-sized blocks in unit 1A (Table 2) would have been fully supported, although this result is strongly dependent on the estimated shear strength of the sediments (see Naylor, 1982). Another important result is that as block size increases, as measured by thickness, the block must take on a more tabular shape to avoid sinking into the underlying sediments. For example, given the case in Figure 13, fully supported blocks with thicknesses of 1 m could have a variety of shapes because the minimum required aspect ratio is 2, whereas a 5-m-thick block would have to have a highly tabular shape to remain fully supported because the minimum aspect ratio is 6. Blocks in unit 1A definitely show a relationship of increasing aspect ratio with block thickness. The prevalence of stable blocks in unit 1A may be due to the sliding process because statically stable blocks would have been capable of sliding the greatest distance.

UNIT 1B: MUDSTONE-SANDSTONE MÉLANGE WITHOUT EXOTIC BLOCKS

Unit 1B represents the second type of mélangé within unit 1. The south limb of the Ucluth anticline exposes a complete section of unit 1B, where it dips moderately to the south and has an estimated thickness of 1,000 to 1,500 m. The lower third of this section is particularly well exposed in the Big Beach area, which was mapped in detail (Fig. 14) to illustrate the internal structure and stratigraphy of the unit.

Unit 1B is best described as a stratally disrupted sedimentary sequence or a broken formation, rather than a blocks-in-matrix mélangé. It consists of a chaotic assemblage of four sedimentary units (relative proportions in percent): (1) black mudstone, typically laminated, with calcareous concretions and rare sandstone interbeds (50%); (2) medium- to thick-bedded turbidites with minor channeled bodies of clast-supported, chert-pebble conglomerate (45%); (3) pebbly mudstone (5%); and (4) rare radiolarian ribbon chert (<1%). Interbedded relationships are found between all of these units (see Fig. 14 for examples), indicating that they were derived from a single stratigraphic sequence. Again, it is important to stress that the ribbon chert is not exotic. It forms well-bedded horizons (0.5 to 7 m thick) within sandstone-rich turbidite sequences (for example, see right side of Fig. 14). These cherts commonly contain sandy chert interbeds, much like those found in unit 1A, attesting to their depositional association with the surrounding clastic sediments.

Unit 1B lacks exotic or extraformational blocks, with the exception of clasts found in pebbly mudstones, such as the 90-m-thick sequence exposed on the north side of Big Beach (Fig. 14). The pebbly mudstones are matrix-supported conglomerates, which were probably deposited as submarine debris flows. They contain well-rounded clasts of volcanic rock (Fig. 15a), predominantly tuff and tuff breccia, with minor flow rock. The clasts resemble fragmental volcanic rocks in the Ucluth Formation and may have been derived from there. Clast size typically ranges from granule to boulder (Fig. 15a), but larger blocks, as much as 4 m across, are also locally present (Fig. 15b). Fossils from unit 1B indicate an Early Cretaceous age (Table 1). *Buchia* of early or middle Valanginian age are present at a number of localities in mudstone of the mélangé. Typically, they form rare interbeds (coquina) composed entirely of re-worked shells. Three radiolarian localities from ribbon chert interbedded with turbidites and mudstones indicate a late Valanginian or early Hauterivian age, similar to the *Buchia*.

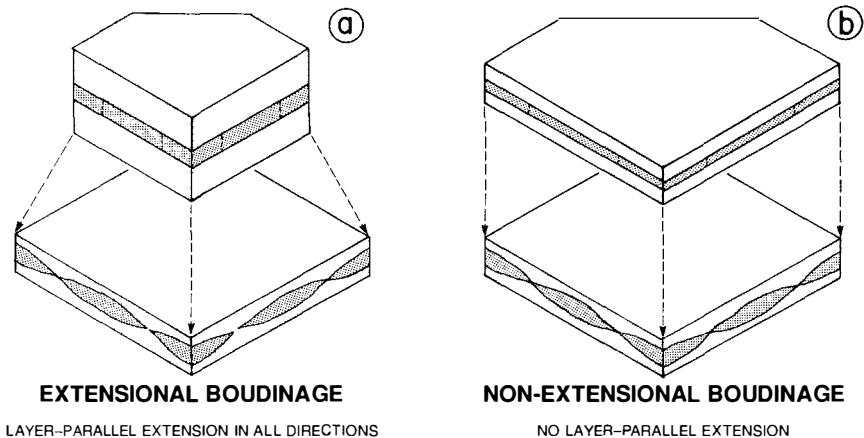


Figure 12. Two processes that can produce boudin-like structures, such as those observed in unit 1A. (a) Extensional boudinage with bulk extension occurring in all directions parallel to layering. (b) A nonextensional form of boudinage caused by lateral flowage and thickening of the sand layer, in the absence of bulk layer-parallel extension. Note that unlike these idealized examples, the boudin-like structures in unit 1A are highly irregular in shape and in spacing (for example, Figs. 8d and 9).

Internal Structure

In contrast to unit 1A, the sedimentary units that make up unit 1B generally have retained their stratal coherence. Bedding and primary

deposition structures are almost everywhere well preserved. The most visible effects of mélangé deformation are a confused style of folding, characterized by highly variable bedding attitudes, many of which are overturned

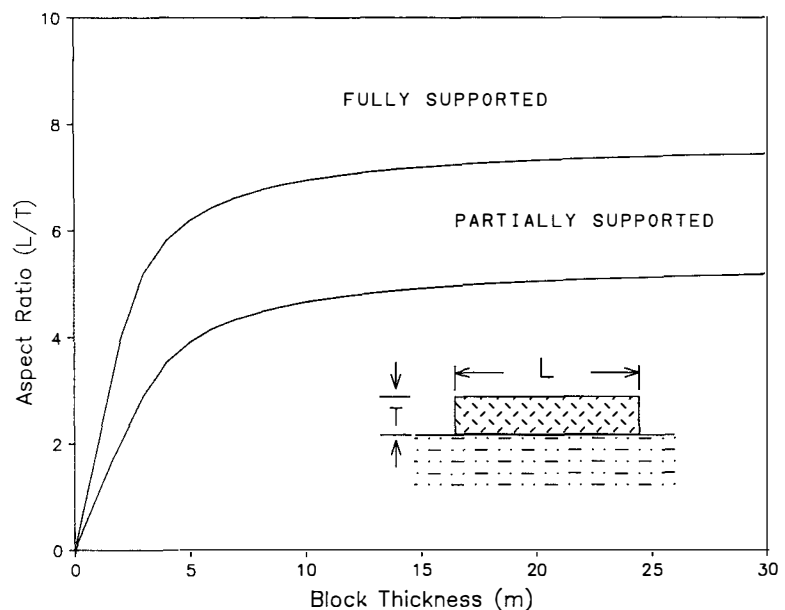


Figure 13. Static stability of a block resting on muddy sea-floor sediments. This graph illustrates that blocks of appropriate dimensions can rest fully supported on the sea floor without sinking into the underlying mud. Furthermore, thick blocks (>5 m) must have relatively large aspect ratios (>7) to remain fully supported. Blocks are approximated as a circular column having a diameter of L and a height of T ; the various stability fields are calculated using equations and material properties from Naylor (1982). Undrained loading is assumed to simulate rapid emplacement of the block.

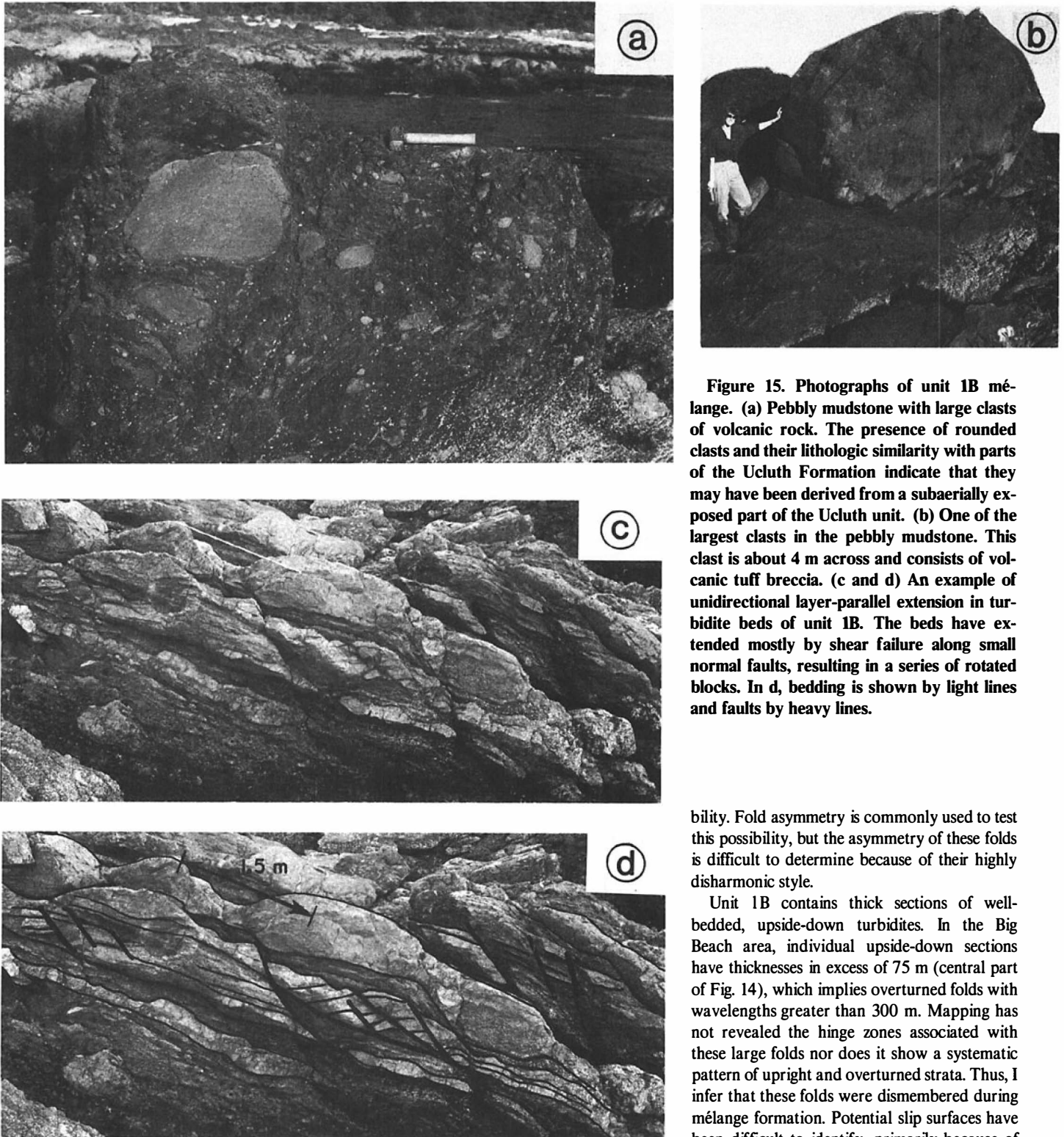


Figure 15. Photographs of unit 1B mélange. (a) Pebbly mudstone with large clasts of volcanic rock. The presence of rounded clasts and their lithologic similarity with parts of the Ucluth Formation indicate that they may have been derived from a subaerially exposed part of the Ucluth unit. **(b)** One of the largest clasts in the pebbly mudstone. This clast is about 4 m across and consists of volcanic tuff breccia. **(c and d)** An example of unidirectional layer-parallel extension in turbidite beds of unit 1B. The beds have extended mostly by shear failure along small normal faults, resulting in a series of rotated blocks. In d, bedding is shown by light lines and faults by heavy lines.

(Figs. 10b and 14). In the Big Beach area, poles to bedding form a crude girdle pattern (Fig. 10b), indicating folding around an east-trending, moderately plunging axis. At outcrop scale, however, there is little evidence of conventional fold patterns. The more thinly bedded strata are contorted into highly disharmonic folds, with

limb angles ranging from open to tight and amplitudes of 1 to 10 m. These folds lack a consistent orientation (Fig. 10c) and show no obvious relation to the best-fit map-scale fold axis, as defined by poles to bedding (Fig. 10b). The folds may mark the presence of diffuse shear zones, which would account for their geometric varia-

bility. Fold asymmetry is commonly used to test this possibility, but the asymmetry of these folds is difficult to determine because of their highly disharmonic style.

Unit 1B contains thick sections of well-bedded, upside-down turbidites. In the Big Beach area, individual upside-down sections have thicknesses in excess of 75 m (central part of Fig. 14), which implies overturned folds with wavelengths greater than 300 m. Mapping has not revealed the hinge zones associated with these large folds nor does it show a systematic pattern of upright and overturned strata. Thus, I infer that these folds were dismembered during mélangé formation. Potential slip surfaces have been difficult to identify, primarily because of poor exposure in critical areas. One well-exposed example (center of Fig. 14, at fold plunging 61°) consists of a 2-m-thick disturbed zone marked by a rootless anticline (1.5 m amplitude, 30° limb angle). There is no indication of the magnitude or sense of slip.

In a few cases, sandstone beds have been extended parallel to layering (Figs. 15c and 15d).

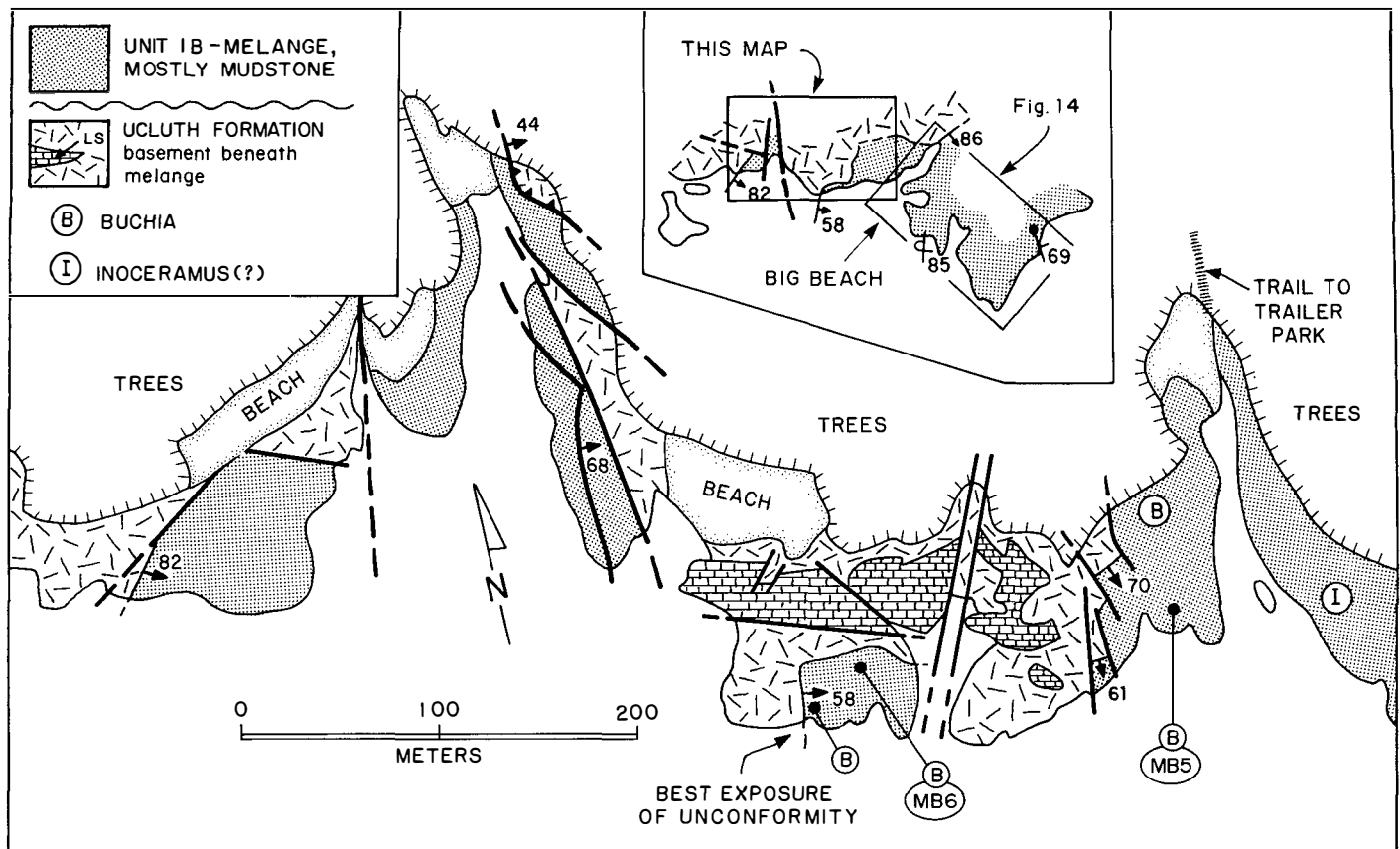


Figure 16. Outcrop map showing the basal unconformity of unit 1B on the Ucluth Formation. The inset shows the location of the map. The unconformity is offset and repeated by a number of steep faults, so that it helps to refer to the schematic version of the contact shown in the inset. Strata above the unconformity consist of mudstone-rich mass-wasting deposits with ubiquitous *Buchia*. Numbers (for example, MB5) refer to fossil localities in Table 1.

Some beds have extended by necking, resulting in lenticular boudins, whereas others have extended along small normal faults, forming discrete rotated blocks (compare with extensional shear fracture in Cowan, 1982a). Unlike unit 1A, these beds have been pulled apart in only one direction. Furthermore, they have retained their internal sedimentary structures, indicating a relatively brittle style of deformation, without wholesale flowage and thickening.

The unit 1B mélangé is inferred to have formed prior to lithification of the mélangé sediments. The main evidence for this conclusion is that folding occurred without the development of a cleavage. Thin sections of deformed sandstone and mudstone display little if any cataclasis, indicating that strains were accommodated by particulate flow. Unit 1B does contain a sporadically developed spaced cleavage, especially in more mudstone-rich parts of the unit. This cleavage cuts obliquely across the outcrop-scale folds described above and thus appears to post-date folding. The presence of insoluble residues

along cleavage surfaces and the absence of metamorphic recrystallization indicate formation by pressure solution after lithification. The sporadic and semi-penetrative nature of the cleavage indicates only minor strains during cleavage formation.

Unconformity beneath Unit 1B

Based solely on the observations above, the interpretation of unit 1B would remain ambiguous. The mélangé could be ascribed to tectonic processes, such as folding and imbrication of unlithified sediments at a subduction thrust, or to surficial mass wasting, involving folding and faulting within one or more submarine slumps. The main evidence favoring the latter interpretation is the presence of a stratigraphic contact between unit 1B and the underlying Ucluth Formation.

This unconformity is best exposed a short distance west of the Big Beach map area (Fig. 16). As shown in the inset in Figure 16, the contact

strikes through a very poorly exposed part of the Big Beach map area (northwest corner, near the trail) and then continues westward to the coast where it is well exposed at low tide. The unconformity is offset and repeated by a number of high-angle faults, with both right- and left-lateral separation. In general, the unconformity dips moderately to the south, although the surface shows considerable local relief (about 1 to 2 m). At the contact, volcanic rocks of the Ucluth Formation are positionally overlain by a massive, *Buchia*-bearing mudstone, probably a debris-flow deposit. There is no evidence of local faulting or shearing. About 10 to 20 m above the contact, the massive mudstone passes into a highly contorted laminated mudstone with several prominent beds of *Buchia coquina*; the fossils themselves are not noticeably deformed.

My interpretation is that this contact marks an unconformity between lower Mesozoic volcanic rocks and an overlying stratigraphic sequence of Early Cretaceous slumps and debris

flows. Thus, the Ucluth Formation is viewed as depositional basement to the Pacific Rim mélanges. A potential objection to this interpretation centers on the possibility that the Ucluth Formation in the core of the Ucluth anticline may represent a large mélange block of either olistostromal or tectonic origin. This block would have to be very large to encompass the 4 km of Ucluth outcrop exposed in the anticline. An olistostromal slide block of this size, although not impossible, is considered unlikely. I do not dispute the other alternative, that at some scale, the Ucluth rocks form part of a large tectonic block or fault slice. Even so, the unconformity between the mélange and the Ucluth Formation must still be accounted for.

Paleoecological Implications of *Inoceramus*?

Some paleoecological information about the basin from which the slumps and debris flows originated is provided by the *in situ* presence of a large bivalve, which is ubiquitous in unit 1B (labeled "*Inoceramus*?" in Figs. 14 and 16). This fossil, which ranges to as much as 175 cm across, is generally found in growth position (reclined, parallel to bedding) in laminated mudstones and in mudstone interbeds of the turbidites. E. G. Kauffman (1983, personal commun.) examined these fossils and concluded that they represent large inoceramid-like bivalves (see appendix for details). Although their genus and species is unknown, Kauffman stated that they probably occupied the same habitats as some of the larger species of Cretaceous *Inoceramus*, based on similarities in size, morphology, and reclining form (see Kauffman and others, 1977; Jablonski and Bottjer, 1983; and references cited therein).

This conclusion leads to the following inferences. The first is that strata in unit 1B were derived from a relatively shallow basin. Thiede and Dinkelman (1977) reviewed the paleobathymetric range of the numerous *Inoceramus* finds in upper Mesozoic strata cored by the Deep Sea Drilling Project. They concluded that the *Inoceramus* habitat was restricted to less than 2 km water depth, implying a similar depth range for the large bivalves in unit 1B (E. G. Kauffman, 1983, personal commun.). The second inference is that the bottom water in this basin was poorly oxygenated. Kauffman and others (1977) showed that a benthic fauna composed of solitary large inoceramids is indicative of dysaerobic bottom water (also see Savrda and Bottjer, 1987). Unit 1B contains a similar restricted fauna (*Buchia* are allochthonous). Other evidence of dysaerobic conditions in unit 1B is the near absence of trace fossils (Byers, 1977) and the common presence of calcareous concre-

tions (Johnson, 1978). The mudstones are not highly organic (0.2% to 0.9% organic carbon for 6 samples), which implies that oceanographic factors, at least in part, were responsible for this poorly oxygenated condition.

Interpretation of Unit 1B

To summarize, unit 1B is considered a stratigraphic accumulation of mass-wasting deposits, formed primarily by submarine slumping. The source of these slumps is inferred to be an intra-slope basin located at a continental margin. Continental-rise and abyssal-plain settings are unlikely, because they generally lie in water depths greater than 2 km, the maximum depth for the *Inoceramus* habitat. Evidence of dysaerobic bottom water suggests that this basin may have been situated in the oxygen minimum zone, which in the modern oceans, intersects the continental slope at a water depth of about 100 to 1,500 m (Kennett, 1982, p. 236).

This intra-slope basin was probably filled by a submarine fan that included turbidites, channeled conglomerates, and mud-rich interchannel deposits (laminated mud). The pebbly mudstones may have been deposited at the perimeter of this basin or may have formed at a later time in association with downslope movement of the basal strata.

The unconformity beneath unit 1B represents an important stratigraphic hiatus that formed by nondeposition or by uplift and erosion of the underlying Ucluth Formation. Accumulation of unit 1B above this unconformity implies Early Cretaceous subsidence of the Ucluth. The presence of rounded volcanic clasts in pebbly mudstone deposits suggests that other parts of the Ucluth may have been subaerially exposed at that time.

UNIT 2: SANDSTONE-RICH MÉLANGE WITHOUT EXOTIC BLOCKS

Unit 2 is the stratigraphically highest unit in the Pacific Rim Complex. It consists of a disrupted sand-rich turbidite sequence, composed primarily of massive sandstone, with subordinate medium- to thick-bedded turbidites and minor channeled conglomerate (clast supported). In many respects, this mélange is similar to unit 1B, except for the relative proportions of sandstone and mudstone. Unit 2 contains more than 90% sandstone.

The best exposures of unit 2 are located in the northern part of the Pacific Rim Complex along the south side of Vargas Island and the southwest side of the Esowista Peninsula (Fig. 8). The Esowista-Vargas Island area provides some 20

km of coastal outcrop, which was used to study the internal structure of the unit. Unfortunately, contacts with other Pacific Rim units are either unexposed or badly faulted there. More limited exposures of unit 2, located in the south flank of the Ucluth anticline (Fig. 4), indicate that it stratigraphically overlies unit 1B. The contact is marked by a gradual increase in the proportion of sandstone toward the south.

Unit 2 has not yielded fossils, but its gradational relationship with unit 1B implies a similar Early Cretaceous age. The thickness of unit 2 is not known, but the fact that it occupies roughly the same amount of outcrop area as unit 1 suggests that its present exposed thickness may be similar (about 500 to 1,500 m).

Internal Structure

At map scale, unit 2 is distinguished by a highly disorganized pattern of upright and overturned beds (Fig. 10d). At outcrop scale, however, there is little evidence of deformation. Bedding and internal depositional structures are all well preserved, and a spaced cleavage is only locally developed in mudstone interbeds. Small symmetric folds, with amplitudes of 1 to 3 m and tight to isoclinal limb angles, are locally present, but only eight such folds were found in the Esowista-Vargas Island area. Figure 10e shows that they lack a common orientation.

At map scale, strata are organized into discrete depositional sequences, each of which has a thickness of about 100 to 200 m and is distinguished by a relatively consistent bedding orientation and younging direction. In one exceptional case, a sequence composed of moderately dipping, overturned strata has a minimum thickness of 375 m (Fig. 21 in Brandon, 1985). Although only locally exposed, the boundaries between these sequences appear to correspond to discrete slip surfaces, which mark abrupt changes in bedding orientation. The slip surfaces are not brittle faults and thus are inferred to have formed prior to lithification of the turbidites.

Interpretation of Unit 2

One possible explanation for the internal structure of this mélange is that differential rotation between the depositional sequences was due to movement along listric-shaped slip surfaces. Overturning of these thick sequences is difficult to explain by this process alone. Thus, I conclude that like unit 1B, this mélange formed by dismemberment of a series of overturned folds. Both of these structures, the slip surfaces and the folds, may have formed within the frontal part of one or more submarine slump sheets. The general absence of cleavage and the seemingly

chaotic scatter of bedding attitudes and fold orientations are compatible with a near-surface deformational setting. By analogy with unit 1B, the source area for these slumps is inferred to have been an intra-slope turbidite basin.

DISCUSSION

Pacific Rim Mélanges: A Product of Mass Wasting

The main deformational features of the Pacific Rim mélanges, which included layer-parallel fragmentation, obliteration of primary sedimentary structures, emplacement of exotic blocks, and the formation of tight folds and overturned beds without an associated cleavage, are considered to be a result, either directly or indirectly, of widespread surficial mass wasting. These same features are common in many other sediment-rich mélanges, including those of presumed olistostromal and tectonic origins. At present, there is little general agreement about how these structures form. For instance, Cloos (1984) argued that exotic blocks in mudstone-rich Franciscan mélanges were derived by a highly mobile mud matrix that plucked blocks from depths as great as 25 km and carried them to the surface. In contrast, Page and Suppe (1981), Naylor (1982), and Phipps (1984) concluded that similar blocks-in-matrix mélanges in Taiwan, California, and the Apennines formed by surficial debris flows and rock slides. A similar range of interpretations has been proposed for layer-parallel fragmentation, such as (1) lateral spreading within a surficial mass flow (Cowan, 1982a, 1985), (2) boudinage and faulting within a tectonic shear zone (Byrne, 1984; Bosworth, 1984), and (3) *in situ* liquefaction resulting in nonextensional fragmentation and thickening (proposed herein; Fig. 12b).

This lack of consensus is the result of two fundamental problems. The first is the absence of an experimentally based constitutive model capable of describing the deformational behavior of poorly lithified, water-saturated sediments under relevant geologic conditions. As a result, it is hard to assess the mechanical feasibility of various structural interpretations. The second problem concerns uncertainties in the relative timing of different structures within a mélange. For instance, many workers have concluded that formation of a mélange, as marked by stratal disruption and/or intermixing of exotic blocks, is synchronous with development of a scaly cleavage or formation of brittle-style thrust faults. If correct, the mélange is probably of tectonic origin, but synchrony is difficult to prove. The alternative is a polygenetic origin (for example, Aalto, 1986) involving surficial mass wasting and subsequent tectonic deformation. In order to circumvent these problems, my inter-

pretations rely heavily on stratigraphic evidence and also on observations from areas where superposed deformation, such as faults and cleavage, is minimal.

A common objection to the olistostromal interpretation is the apparent absence of modern analogues. Recent marine surveys, however, especially those employing sidescan swath mapping, indicate that submarine mass wasting is much more widespread than previously appreciated and can occur in a variety of tectonic settings (for example, Atlantic continental margins: Damuth and Embley, 1981; Jacobi, 1984; Embley and Jacobi, 1986; Gulf Coast shelf: Prior and Coleman, 1982; northern California shelf: Field and others, 1982). Recently published sidescan swath maps (Davis and others, 1987) covering the continental slope and rise of the Vancouver Island subduction zone and the Queen Charlotte transform fault show widespread mass wasting. Mass-wasting deposits account for about 10% of the surface sediments on the lower slope of the Vancouver Island margin. Individual deposits range to as much as 180 km² in size and contain blocks more than 100 to 200 m across.

Underwood (1984) noted an important paradox of the olistostromal interpretation. Most sediment-rich mélanges contain turbidite sequences that were deformed and incorporated into the mélanges while still in an unlithified state. He argued that these mélanges could not have formed by mass wasting because turbidite deposition requires a relatively flat-lying basinal setting. In other words, how can extensive downslope movement occur in an area with little or no surface slope?

If the olistostromal interpretation is correct for the Pacific Rim mélanges, then the only reasonable explanation is that mass wasting was caused by frequent large earthquakes, presumably at a seismogenic plate boundary (see Schwarz, 1982, for a review of submarine slope failure). Rapid sedimentation may also result in extensive mass failure in areas with gentle surface slopes, but this phenomenon is largely restricted to settings with very high sedimentation rates, such as the Mississippi delta (average of 1 m/yr; Prior and Coleman, 1982). The association of earthquakes with large mass failures is well established (for example, Field and others, 1982; Schwarz, 1982; Keefer, 1984; Piper and others, 1985; and many others). In some cases, the earthquake merely acts as a triggering agent; however, more commonly, it represents the underlying cause of failure because prolonged seismic shaking produces large transient pore pressures in loosely compacted, near-surface sediments (Seed, 1968, 1976; Seed and Idriss, 1971). As a result, deformation and failure can be induced in areas with very gentle, and even horizontal, surface slopes. The origin of these

transient pore pressures has received considerable attention in soil mechanics (for example, Castro, 1975; Seed, 1976; Castro and Poulos, 1977; Sangrey and others, 1978; Wood, 1982). A brief summary is given here because it provides some insights as to how the various Pacific Rim mélanges may have formed.

Earthquakes, Transient Pore Pressures, and Mass Failure

The pore-pressure response of sediments during an earthquake is experimentally studied by applying a rapidly alternating cyclic load (simulating ground shaking) to a water-saturated test sample under undrained conditions, that is, pore fluid is not allowed to leave the sample. The resulting excess pore pressure is compared to excess pore pressures developed under an equivalent static load; the difference is termed "anomalous excess pore pressure." These experiments have shown that the largest anomalous excess pore pressures are produced in loose silt and sand because they have a relatively stiff elastic response and because they tend to compact when loaded (Egan and Sangrey, 1978; Sangrey and others, 1978). Furthermore, sand and silt require much smaller cyclic shear stresses relative to mud to initiate this anomalous-pore-pressure behavior (25% of normal undrained strength for sand, and 70% for mud). Regardless of sediment type, the transient increase in pore pressure during cyclic loading causes a decrease in the effective strength of the sediment, possibly resulting in ground failure. Liquefaction represents an extreme case, where pore pressure becomes equal to the mean total stress (Castro, 1975; Seed, 1976), at which point the granular aggregate no longer has any shear strength. Silts and sands are most prone to liquefaction because they are capable of rapidly generating the necessary pore pressures.

Under geologic conditions, a number of other factors are important in determining the maximum pore-pressure response and the type of ground failure during an earthquake (Seed and Idriss, 1971; Seed, 1976). Obvious factors are the duration and intensity of ground shaking, which are dependent, in part, on earthquake magnitude and distance to the epicenter. Another factor is the maintenance of high pore pressures. For instance, units composed entirely of very fine sand or silt or of interbedded sand and mud would be highly susceptible to liquefaction because they combine low permeability with high pore-pressure potential. Another factor is the gradient of the surface slope; the highest excess pore pressures are developed in sediments with the *lowest* surface slope, when other factors are equal (Seed, 1976; Egan and Sangrey, 1978). As a result, sediments in level-ground areas are the most susceptible to lique-

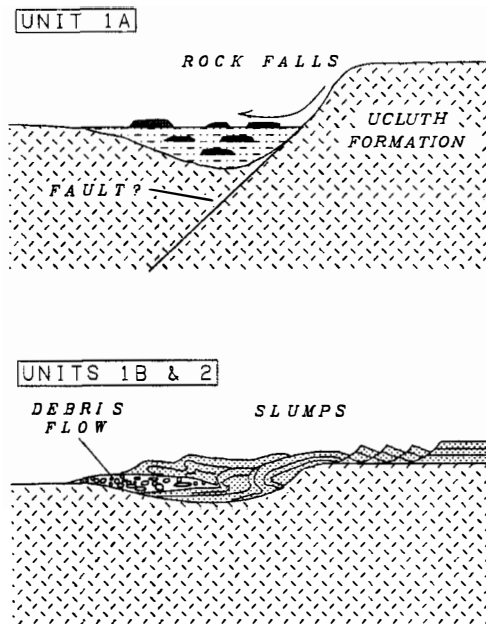


Figure 17. Cross sections illustrating some geologic settings in which the Pacific Rim mélanges may have formed.

faction, whereas sediments in sloping areas tend to fail by slumping or sliding (that is, shear failure), before they reach their maximum pore-pressure potential. There is also a depth-dependent effect. Pore pressures large enough to cause liquefaction tend to occur only in near-surface sediments, probably no deeper than 15 m (Seed, 1968).

Geologic Setting of Mélange Units

The deformational behavior of sediments during earthquake shaking can account for the structural differences among the mélange units in the Pacific Rim Complex. Unit 1A is characterized by a well-layered fabric, by layer-parallel fragmentation, and by an absence of primary sedimentary structures in sandstones, whereas units 1B and 2 are characterized by a highly disordered structural style consisting of large dismembered folds, overturned turbidite sequences, and well-preserved sedimentary structures. The difference between these two types of mélange is attributed to differences in surface slope and type of mass failure, as schematically illustrated in Figure 17.

Disruption of the matrix of unit 1A is ascribed to *in situ* liquefaction and flowage of coarse-grained sediments in a mud-rich basal sequence (Fig. 17a). The combination of a level-ground setting and a predominance of mud would have provided ideal conditions for seismically induced liquefaction of the interbedded sandy sediments. Because liquefaction is restricted to near-surface sediments, deposition of the basal sequence must have coincided with a series of large earthquakes in order to produce a pervasively disrupted mélange. Exotic blocks in this mélange were apparently derived as rock

falls from nearby basement scarps. These scarps may have been associated with the seismically active faults responsible for liquefaction.

In contrast, units 1B and 2 are interpreted to have originated by shear failure and downslope mass movement of large slump sheets (Fig. 17b). The preservation of sedimentary structures indicates that liquefaction was not important in these mélanges. Thick sections of overturned strata indicate significant transport, which would require the presence of at least a small downslope gradient. The extensive involvement of basal strata implies that the slumps were derived by retrogressive slumping. In this type of slumping, the headwall scarp migrates rearward into the basin so that the size of the slide increases with time. This process can happen slowly over a period of years or quickly as it did in the submarine slide at Valdez during the 1964 Alaska earthquake (Seed, 1968). The absence of exotic blocks in units 1B and 2 suggests that basement rocks were not exposed in the source areas of these slumps.

Proposed Tectonic History

Most tectonic syntheses of the Pacific Northwest have relied heavily on the interpretation that the Pacific Rim Complex marks the trace of a late Mesozoic subduction zone formed along the western margin of Vancouver Island. The interpretation I prefer is that the Pacific Rim Complex is a displaced terrane, offset during latest Cretaceous or early Tertiary time from an original position about 220 km to the southeast (Brandon, 1985, 1989a). Thus, the origin of the unit may be unrelated to its present tectonic position along the west coast of Vancouver Island.

This interpretation rests on two observations.

First, the faults that presently bound the Pacific Rim Complex seem to be younger than the formational age of the unit. For instance, the West-coast fault, which separates the Pacific Rim Complex from Wrangellia, juxtaposes rocks with sharp contrasts in Mesozoic stratigraphy (Brandon, 1989a) and metamorphic history (discussed below). The fault itself, where exposed in coastal outcrops at the southeast end of the map area, forms a sharp, near-vertical break between Jurassic plutonic rocks of Wrangellia (Westcoast Complex; Isachsen, 1987) and mudstone-rich mélange with volcanic blocks. The fault lies in the middle of a 400-m-wide shear zone characterized by closely spaced (≈ 1 m) brittle-slip surfaces, generally with steep dips, and abundant silica-carbonate alteration. The deformational character of this fault is unique in the map area and is taken as evidence of large amounts of displacement.

The oldest link across the Westcoast fault is provided by a lower Eocene suite of dikes and stocks that were emplaced on both sides of the fault. Small intrusions with early Tertiary ages (55–36 m.y.) are common on Vancouver Island (Armstrong, 1988), but the oldest intrusions (48 to 52 m.y. old) are localized in the Pacific Rim area where they coincide with a coeval tuff breccia, the Flores dacite (Fig. 2). Swarms of subvertical dikes are found throughout the Pacific Rim Complex and also in the adjacent Wrangellia terrane (Isachsen, 1987). These dikes are related to the 50 Ma volcanic-plutonic suite because they radiate from dated intrusions, such as the 52 Ma Tofino pluton (Fig. 2), and because they intrude into the Flores dacite and also cut the basement on which the Flores rests. The main conclusion is that although none of these lower Eocene units cuts or overlies the Westcoast fault, the fact that this igneous activity extended across the fault seems to preclude major displacements after 50 Ma.

The second observation for transcurrent offset is the similarity of the Pacific Rim Complex to parts of the San Juan–Cascades nappes (Fig. 2), which represent a major thrust belt that formed during Late Cretaceous time when Wrangellia collided with the American continent (Brandon and others, 1988; Brandon, 1989b). In the San Juan Islands, these nappes contain rock units that could be equivalent to parts of the Pacific Rim Complex, such as the upper Mesozoic mélanges of the Constitution Formation and Lopez Complex, Upper Jurassic ophiolitic rocks of the Fidalgo Complex, and Upper Triassic arc-volcanic rocks of the Haro Formation (see Brandon, 1989a, for details). More important, however, is that both the Pacific Rim Complex and the San Juan–Cascades nappes were affected by a similar high-pressure metamorphic event that produced the characteristic assemblage prehnite \pm lawsonite \pm aragonite. Brandon

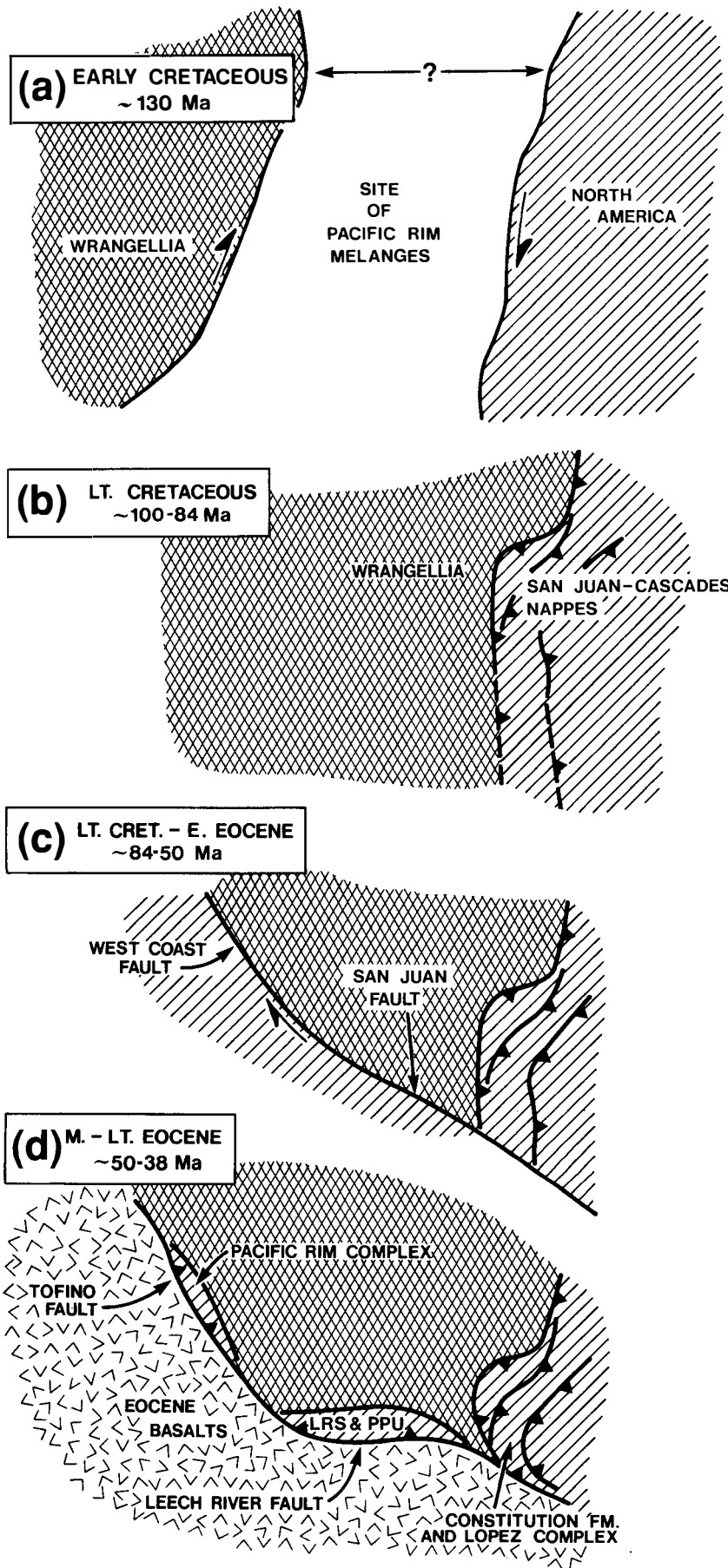


Figure 18. Proposed tectonic history of the Pacific Rim Complex. (a) The Pacific Rim mélanges are formed in a poorly defined zone that used to lie between the Wrangellia terrane of Vancouver Island and the American continent. (b) Wrangellia collides with America. The Pacific Rim Complex is deformed and metamorphosed within the collision zone, marked by the San Juan-Cascades nappes. (c) The southwestern side of Wrangellia and the San Juan-Cascades nappes are truncated by a major transcurrent fault, marked by the trace of the San Juan and West Coast faults. The Pacific Rim Complex, Pandora Peak unit (PPU), and Leech River schist (LRS) are displaced northwestward to their present positions along the southwestern perimeter of Wrangellia. (d) A large, coherent terrane of Eocene basalts is thrust beneath the margin along the trace of the truncation scar. This event marks the initiation of the modern convergent-margin regime.

and others (1988) showed that for the San Juan nappes, high-pressure metamorphism occurred during the interval 100 to 84 Ma and was directly related to formation of the thrust belt. With the exception of the Pacific Rim and related rocks, the San Juan-Cascades nappes represent the only place in the world where prehnite has been found coexisting with lawsonite or aragonite. The uniqueness of this assemblage may be due to rapid vertical transport rates (≈ 2.2 km/m.y.) during thrusting (Brandon and others, 1988).

In the vicinity of Vancouver Island, prehnite-lawsonite assemblages are restricted to the displaced Mesozoic rocks that border the southern and western perimeter of Wrangellia (Fig. 2). Aragonite has not been found in these rocks, but it inverts quickly at temperatures in excess of 75 to 100 °C (Carlson and Rosenfeld, 1981) and thus would have been obliterated by Tertiary igneous activity in the Vancouver Island area (Armstrong, 1988). My work indicates that prehnite-lawsonite assemblages are present throughout the Pacific Rim Complex but are absent in directly adjacent rocks of the Wrangellia terrane. Rusmore and Cowan (1985) have reported a similar relationship in the Pandora Peak unit (PP in Fig. 2), a mélangé unit that is directly equivalent to the Pacific Rim Complex. Furthermore, they can show that the fault contact between Pandora Peak and Wrangellia postdates high-pressure metamorphism. This evidence suggests that the San Juan and West Coast faults (Fig. 2) postdate 84 Ma, which marks the end of metamorphism in the San Juan Islands.

The proposed tectonic history of the Pacific Rim Complex is illustrated in Figure 18. The

first stage marks the formation of the Pacific Rim mélanges during Valanginian and early Hauterivian time (138 to 128 Ma). The mélanges are inferred to have formed in a poorly understood tectonic zone that used to lie between Wrangellia and the American continent. This time marks a widespread lull in arc magmatism along the entire extent of western North America, including Wrangellia (about 155–120 Ma in western Canada: Armstrong, 1988; 147–121 Ma for California: Page and Engebretson, 1984). For this reason, I infer that the Pacific Rim mélanges formed in a continental transform setting, perhaps like the offshore Borderlands of southern California (Gorsline and Emery, 1959; Field and Edwards, 1980). The Borderlands region consists of a complex array of highstanding basement blocks separated by intervening basins. Some basins are connected by submarine channels and are actively accumulating sand-rich turbidites, whereas others are more isolated and are being filled by hemipelagic mud and mass-movement deposits. The Pacific Rim mélanges record a similar range of depositional settings.

The next stage is the Late Cretaceous (100 to 84 Ma) collision of Wrangellia with the American continental margin (Brandon and others, 1988). The San Juan–Cascades thrust system formed within the intervening collision zone. At that time, the Pacific Rim Complex and Pandora Peak unit would have been located at the southern end of this collisional zone, adjacent to the San Juan Islands. It is important to note that the Pacific Rim mélanges were already 30 m.y. old at the time of collision.

The next event, which occurred sometime during latest Cretaceous or early Tertiary time (84 to 50 Ma), involved dextral offset of the southwest continuation of Wrangellia and the San Juan–Cascades thrust system. Large displacement removed this more westerly block from the Vancouver Island area and left behind a truncation scar, roughly coinciding with the San Juan and Westcoast faults. The Pacific Rim Complex and Pandora Peak unit would represent large fault slices that were left stranded along this truncation scar.

The last event, which occurred during Eocene time (55 to 34 Ma), involved northeastward underthrusting of the Eocene basalt terrane beneath this newly truncated edge. Much of this deformation was accommodated by displacement on the Leech River, Tofino, and San Juan faults (Clowes and others, 1987), which were active as late as 40 Ma (Fairchild and Cowan, 1982; Rusmore and Cowan, 1985). This event marks the final assembly of the forearc basement that underlies the modern convergent margin. Upper Eocene and Oligocene strata of the Tofino and Makah basins (Tiffin and others, 1972; Snavely and others, 1980) provide the overlap

sequence that ties all the basement terranes together, including the Eocene basalts.

The present location of the offset block may be southern Alaska. Part or all of the Wrangellia terrane in southern Alaska (Jones and others, 1977) may have been offset from Vancouver Island Wrangellia. The Pacific Rim Complex is strikingly similar to several units within the Chugach terrane: the Uyak Complex of Kodiak Island (Connelly, 1978), the Yakutat Group of southeastern Alaska (Plafker, 1967; also descriptions in Johnson and Karl, 1985), and the Sitka graywacke and Kelp Bay Group of Chichagof and Barnoff Islands (Loney and others, 1975; Johnson and Karl, 1985). Several papers (for example, Cowan, 1982b; Moore and others, 1983; Coe and others, 1985) have already postulated that parts of southern Alaska were transported from more southerly locations during Tertiary time. At present, the stratigraphic, deformational, and metamorphic histories of these units, especially those in the Chugach terrane, are not resolved well enough to warrant a more detailed comparison with Vancouver Island geology. The offset hypothesis, however, makes specific predictions about the geologic composition and tectonic history of the proposed offset block. Thus, it should be possible to uniquely identify this block, if in fact it is present in southern Alaska.

CONCLUDING REMARKS

The Pacific Rim Complex provides an important example of deformational styles developed within a sequence of olistostromal mélanges. Many of the structures in these mélanges are similar to those found in other sediment-rich mélanges of the western Cordillera, including those ascribed to purely tectonic origins. The results of this study indicate that the primary attributes of these types of mélanges, such as pervasive stratal disruption, layer-parallel fragmentation, and the intermixing of exotic blocks, can form in olistostromal mélanges and thus should not be considered diagnostic of a tectonic origin. Other structures, such as scaly cleavage or a network of brittle-style faults, probably do indicate tectonic deformation; however, these structures may be superposed and thus would be unrelated to formation of the mélange. The proposed offset history of the Pacific Rim Complex illustrates how the present structural setting of a mélange may have little bearing on how and where the mélange formed. Other western Cordilleran mélanges may have suffered a similar fate.

ACKNOWLEDGMENTS

This paper is based on Ph.D. research conducted at the University of Washington. D. S. Cowan, S. Monsen, and M. Rusmore contrib-

uted much support and useful discussion throughout the project. Careful reviews by R. A. Schweickert, R. W. Tabor, E. L. Miller, and an anonymous reviewer are greatly appreciated. J. Muller gave access to his unpublished field notes and fossil data. Paleontological identifications were provided courtesy of E. S. Carter, J. A. Jeletzky, E. Kauffman, M. Orchard, E. A. Pessagno, Jr., and E. T. Tozer. Organic carbon analyses were provided by J. I. Hedges. I gratefully acknowledge funding from Sigma Xi, the Geological Society of America, the Department of Geological Sciences Corporation Fund, and the National Science Foundation (Grant EAR81-07654 to D. S. Cowan).

REFERENCES CITED

- Aalto, K. R., 1986, Depositional sequence of argillite, diamictite, hyaloclastite and lava flows within the Franciscan Complex, northern California: *Journal of Geology*, v. 94, p. 744–752.
- Armstrong, R. L., 1988, Mesozoic and early Cenozoic magmatic evolution of the Canadian Cordillera: *Geological Society of America Special Paper* 218, p. 55–91.
- Borradaile, G. J., 1981, Particulate flow of rock and the formation of cleavage: *Tectonophysics*, v. 72, p. 305–321.
- Borradaile, G. J., Bayly, M. B., and Powell, C. McA., eds., 1982, *Atlas of deformational and metamorphic rock fabrics*: Berlin, Germany, Springer-Verlag, 551 p.
- Bosworth, W., 1984, The relative roles of boudinage and "structural slicing" in the disruption of layered rock sequences: *Journal of Geology*, v. 92, p. 447–456.
- Brandon, M. T., 1984, *Deformational processes affecting un lithified sediments at active margins: A field study and a structural model* [Ph.D. thesis]: Seattle, Washington, University of Washington, 159 p.
- , 1985, Mesozoic mélange of the Pacific Rim Complex, western Vancouver Island, in Tempelman-Kluit, D., ed., *Field guides to geology and mineral deposits in the southern Cordillera* (Geological Society of America Cordilleran Section Meeting): Vancouver, British Columbia, Geological Survey of Canada, p. 7.1–7.28.
- , 1989a, Origin of igneous rocks associated with mélanges of the Pacific Rim Complex, western Vancouver Island, Canada: *Tectonics* (in press).
- , 1989b, Geology of the San Juan–Cascade nappes, northwestern Cascade Range and San Juan Islands, in Joseph, N. L., and others, eds., *Geologic guidebook for Washington and adjacent areas*: Washington Division of Geology and Earth Resources Information Circular 86, p. 137–162.
- Brandon, M. T., Cowan, D. S., and Vance, J. A., 1988, The Late Cretaceous San Juan thrust system, San Juan Islands, Washington: *Geological Society of America Special Paper* 221, 81 p.
- Byers, C. W., 1977, Biofacies patterns in euxinic basins: A general model: *Society of Economic Paleontologists and Mineralogists Special Publication* 25, p. 5–17.
- Byrne, T., 1984, Structural geology of mélange terranes in the Ghost Rocks Formation, Kodiak Islands, Alaska: *Geological Society of America Special Paper* 198, p. 21–51.
- Carlson, W. D., and Rosenfeld, J. L., 1981, Optical determination of topotactic aragonite calcite growth kinetics: Metamorphic implications: *Journal of Geology*, v. 89, p. 615–638.
- Carson, D. J. T., 1973, The plutonic rocks of Vancouver Island, British Columbia: Their petrography, chemistry, age, and emplacement: *Geological Survey of Canada Paper* 72-44, 70 p.
- Castro, G., 1975, Liquefaction and cyclic mobility of saturated sands: *American Society of Civil Engineers Journal of the Geotechnical Engineering Division*, v. 101, p. 551–569.
- Castro, G., and Poulos, S. J., 1977, Factors affecting liquefaction and cyclic mobility: *American Society of Civil Engineers Journal of the Geotechnical Engineering Division*, v. 103, p. 501–516.
- Cloos, M., 1984, Flow mélanges and the structural evolution of accretionary wedges: *Geological Society of America Special Paper* 198, p. 71–81.
- Clowes, R. M., Brandon, M. T., Green, A. G., Yorath, C. J., Sutherland-Brown, A., Kanasevich, E. R., and Spencer, C., 1987, LITHOPROBE—Southern Vancouver Island: Cenozoic subduction complex imaged by deep seismic reflections: *Canadian Journal of Earth Sciences*, v. 24, p. 31–51.
- Coe, R. S., Glöberman, B. R., Plumley, P. W., and Thrupp, G. A., 1985, Paleomagnetic results from Alaska and their tectonic implications. in Howell, D. G., ed., *Tectonostratigraphic terranes of the Circum-Pacific region*: Houston, Texas, Circum-Pacific Council for Energy and Mineral Resources, Earth Science Series, v. 1, p. 85–108.
- Connelly, W., 1978, Uyak Complex, Kodiak Island, Alaska: A Cretaceous subduction complex: *Geological Society of America Bulletin*, v. 89, p. 755–769.
- Cowan, D. S., 1982a, Deformation of partly dewatered and consolidated Franciscan sediments near Piedras Blancas Point, California, in Leggett, J. K., ed., *Trench-forearc geology: Sedimentation and tectonics on modern and ancient active plate margins*: Geological Society of London Special Publication 10, p. 439–457.
- , 1982b, Geologic evidence for post-40 m.y. b.p. large-scale northward displacement of part of southeastern Alaska: *Geology*, v. 10, p. 309–313.

- 1985, Structural styles in Mesozoic and Cenozoic mélanges in the western Cordillera of North America: Geological Society of America Bulletin, v. 96, p. 451-462.
- Damuth, J. E., and Embley, R. W., 1981, Mass-transport processes on Amazon Cone: Western Equatorial Atlantic: American Association of Petroleum Geologists, v. 65, p. 629-643.
- Davis, E., Currie, R., and Sawyer, B., 1987, Marine geophysical maps of western Canada, acoustic imagery: Geological Survey of Canada Maps 10-1987, 11-1987, 13-1987, and 15-1987, scale 1:250,000.
- Dickinson, W. R., 1976, Sedimentary basins developed during evolution of Mesozoic-Cenozoic arc-trench system in western North America: Canadian Journal of Earth Sciences, v. 13, p. 1268-1287.
- Egan, J. A., and Sangrey, D. A., 1978, Critical state model for cyclic load pore pressure, in Earthquake engineering and soil dynamics (Volume 1): American Society of Civil Engineering, Geotechnical Engineering Division, Special Conference, Proceedings, p. 410-424.
- Embley, R. M., and Jacobi, R., 1986, Mass wasting in the western North Atlantic, in Vogt, P. R., and Tucholke, B. E., eds., The geology of North America, Volume M, The western North Atlantic region: Boulder, Colorado, Geological Society of America, p. 479-490.
- Fairchild, L. H., and Cowan, D. S., 1982, Structure, petrology and tectonic history of the Leech River Complex, northwest of Victoria, Vancouver Island: Canadian Journal of Earth Sciences, v. 19, p. 1816-1835.
- Field, M. E., and Edwards, B. D., 1980, Slopes of the southern California continental borderland: A regime of mass transport, in Field, M. E., Bouma, A. H., Colburn, I. P., Douglas, R. G., and Ingle, J. C., eds., Quaternary depositional environments of the Pacific Coast: Society of Economic Paleontologists and Mineralogists, Pacific Section, p. 169-184.
- Field, M. E., Gardner, J. V., Jennings, A. E., and Edwards, B. D., 1982, Earthquake-induced sediment failures on a 0.25° slope, Klamath River delta, California: Geology, v. 10, p. 542-546.
- Gorstine, D. S., and Emery, K. O., 1959, Turbidity-current deposits in San Pedro and Santa Monica Basins off southern California: Geological Society of America Bulletin, v. 70, p. 279-290.
- Harland, W. B., Cox, A. V., Llewellyn, P. G., Pickerton, C. A. G., Smith, A. G., and Walters, R., 1982, A geologic time scale: Cambridge, United Kingdom, Cambridge University Press, 131 p.
- Ineson, J. R., 1985, Submarine glide blocks from the Lower Cretaceous of the Antarctic Peninsula: Sedimentology, v. 32, p. 659-670.
- Isachsen, C. E., 1987, Geology, geochemistry and cooling history of the West-coast Crystalline Complex and related rocks, Meares Island and vicinity, Vancouver Island, British Columbia: Canadian Journal of Earth Sciences, v. 24, p. 2047-2064.
- Jablonski, D., and Bottjer, D. J., 1983, Soft-bottom epifaunal suspension-feeding assemblages in the Late Cretaceous—Implications for the evolution of benthic paleocommunities, in Tevesz, M. J. S., and McCall, P. L., eds., Interaction in recent and fossil benthic communities: New York, Plenum, p. 747-812.
- Jacobi, R. D., 1984, Modern submarine sediment slides and their implications for mélange and the Dunnage Formation in north-central Newfoundland: Geological Society of America Special Paper 198, p. 81-102.
- Jenkyns, H. C., and Winterer, E. L., 1982, Paleogeography of Mesozoic ribbon radiolites: Earth and Planetary Science Letters, v. 6, p. 351-375.
- Johnson, B. R., and Karl, S. M., 1985, Geologic map of western Chichagof and Yakobi Islands, southeastern Alaska: U.S. Geological Survey Map 1-1506 with accompanying text, scale 1:125,000.
- Johnson, H. D., 1978, Shallow siliclastic seas, in Reading, H. G., ed., Sedimentary environments and facies: New York, Elsevier, p. 207-258.
- Jones, D. L., and Murchey, B., 1986, Geologic significance of Paleozoic and Mesozoic radiolarian chert: Annual Reviews of Earth and Planetary Sciences, v. 14, p. 435-492.
- Jones, D. L., Silberling, N. J., and Hillhouse, J., 1977, Wrangellia—A displaced terrane in northwestern North America: Canadian Journal of Earth Sciences, v. 14, p. 2565-2577.
- Kauffman, E. G., Hattin, D. E., and Powell, J. D., 1977, Stratigraphic, paleontological and paleoenvironmental analyses of the Upper Cretaceous rocks of Cimarron County, northwestern Oklahoma: Geological Society of America Memoir 149, 150 p.
- Keefer, D. K., 1984, Landslides caused by earthquakes: Geological Society of America Bulletin, v. 95, p. 406-421.
- Kennett, J. P., 1982, Marine geology: Englewood Cliffs, New Jersey, Prentice-Hall, 813 p.
- Kent, D. V., and Gradstein, F. M., 1985, A Cretaceous and Jurassic geochronology: Geological Society of America Bulletin, v. 96, p. 1419-1427.
- Loney, R. A., Brew, D. A., Muffler, L. J. P., and Pomeroy, J. S., 1975, Reconnaissance geology of Chichagof, Baranof and Kruzof Islands, southeastern Alaska: U.S. Geological Survey Professional Paper 792, 105 p.
- MacLeod, N. S., Tiffin, D. L., Snavely, P. D., Jr., and Currie, R. G., 1977, Geologic interpretations of magnetic and gravity anomalies in the Strait of Juan de Fuca, U.S.—Canada: Canadian Journal of Earth Sciences, v. 14, p. 223-238.
- Massey, N.W.D., 1986, The Metochos Igneous Complex, southern Vancouver Island: Ophiolite stratigraphy developed in an emergent island setting: Geology, v. 14, p. 602-605.
- Monger, J.W.H., Price, R. A., and Tempelman-Kluit, D. J., 1982, Tectonic accretion and the origin of two major metamorphic and plutonic belts in the Canadian Cordillera: Geology, v. 10, p. 70-75.
- Moore, J. C., Byrne, T., Plumley, P. W., Reid, M., Gibbons, H., and Coe, R. S., 1983, Paleogene evolution of the Kodiak Islands, Alaska: Consequences of ridge-trench interaction in a more southerly latitude: Tectonics, v. 2, p. 265-293.
- Muller, J. E., 1973, Geology of Pacific Rim National Park: Geological Survey of Canada Paper 73-1A, p. 29-37.
- 1976, Cape Flattery map area (92C), British Columbia: Geological Survey of Canada Paper 76-1A, p. 107-112.
- 1977a, Evolution of the Pacific margin, Vancouver Island, and adjacent regions: Canadian Journal of Earth Sciences, v. 14, p. 2062-2085.
- 1977b, Geology of Vancouver Island: Geological Survey of Canada Open-File Map 463, scale 1:250,000.
- Muller, J. E., Northcote, K. E., and Carlisle, D., 1974, Geology and mineral deposits of Nootka Sound map area, Vancouver Island, British Columbia: Geological Survey of Canada Paper 74-8, 77 p.
- Muller, J. E., Cameron, B.E.B., and Northcote, K. E., 1981, Geology and mineral deposits of Nootka Sound map area, Vancouver Island, British Columbia: Geological Survey of Canada Paper 80-16, 53 p.
- Naylor, M. A., 1982, The Casanova Complex of the northern Apennines: A mélange formed on a distal passive continental margin: Journal of Structural Geology, v. 4, p. 1-18.
- Oertel, G., 1983, The relationship of strain and preferred orientation of phyllosilicate grains in rocks—A review: Tectonophysics, v. 100, p. 413-447.
- Page, B. M., and Engebretson, D. C., 1984, Correlation between the geologic record and computed plate motions for central California: Tectonics, v. 3, p. 133-155.
- Page, B. M., and Suppe, J., 1981, The Pliocene Lichi mélange of Taiwan: Its plate-tectonic and olistostromal origin: American Journal of Science, v. 281, p. 193-227.
- Page, R. J., 1974, Sedimentology and tectonic history of the Esowista and Ucluth Peninsulas, west coast, Vancouver Island, British Columbia [Ph.D. thesis]: Seattle, Washington, University of Washington, 72 p.
- Phipps, S. P., 1984, Ophiolitic olistostromes in the basal Great Valley Sequence, Napa County, northern California Coast Ranges: Geological Society of America Special Paper 198, p. 103-126.
- Piper, D.J.W., Shor, A. N., Farre, J. A., O'Connell, S., and Jacobi, R., 1985, Sediment slides and turbidity currents on the Laurentian fan: Sidescan sonar investigations near the epicenter of the 1929 Grand Banks earthquake: Geology, v. 13, p. 538-541.
- Plafker, G., 1967, Geologic map of the Gulf of Alaska Tertiary province, Alaska: U.S. Geological Survey Miscellaneous Geologic Investigations Map I-484, 1:500,000.
- Prior, D. B., and Coleman, J. M., 1982, Active slides and flows in under-consolidated marine sediments on the slopes of the Mississippi delta, in Saxon, S., and Nieuwenhuis, J. K., eds., Marine slides and other mass movements: New York, Plenum, p. 21-49.
- Prior, D. B., Bornhold, B. D., and Johns, M. W., 1984, Depositional characteristics of a submarine debris flow: Journal of Geology, v. 92, p. 707-727.
- Ramsay, J. G., 1967, Folding and fracturing of rocks: New York, McGraw-Hill, 568 p.
- Rusmore, M. E., and Cowan, D. S., 1985, Jurassic-Cretaceous rock units along the southern edge of the Wrangellia terrane on Vancouver Island: Canadian Journal of Earth Sciences, v. 22, p. 1223-1232.
- Sangrey, D. A., Castro, G., Poulos, S. J., and France, J. W., 1978, Cyclic loading of sands, silts and clays, in Earthquake engineering and soil dynamics (Volume 2): American Society of Civil Engineers, Geotechnical Division, Special Conference, Proceedings, p. 836-851.
- Savirca, C. E., and Bottjer, D. J., 1987, The exarobic zone, a new oxygen-deficient marine biofacies: Nature, v. 327, p. 54-56.
- Schwarz, H. U., 1982, Subaqueous slope failure—Experiments and modern occurrences, in Contributions to sedimentology (Volume 11): New York, Elsevier, 116 p.
- Seed, H. B., 1968, Landslides during earthquakes due to soil liquefaction: American Society of Civil Engineering Journal of the Soil Mechanics and Foundation Division, v. 94, p. 1055-1122.
- 1976, Evaluation of soil liquefaction effects on level ground during earthquakes, in Liquefaction problems in geotechnical engineering: American Society of Civil Engineering Annual Convention and Exposition, Philadelphia, Pennsylvania, Preprint 2752, p. 1-104.
- Seed, H. B., and Idriss, I. M., 1971, Simplified procedure for evaluating soil liquefaction potential: American Society of Civil Engineering Journal of Soil Mechanics and Foundations Division, v. 97, p. 1249-1273.
- Shouldice, D. H., 1971, Geology of the western Canadian continental shelf: Bulletin of Canadian Petroleum Geology, v. 19, p. 405-436.
- Smith, R. B., 1977, Formation of folds, bounding, and nullions in non-Newtonian materials: Geological Society of America Bulletin, v. 88, p. 312-320.
- Snavely, P. D., Jr., Niem, A. R., MacLeod, N. S., Pearl, J. E., and Rau, W. W., 1980, Makah Formation—A deep-marginal-basin sequence of late Eocene and Oligocene age in the northwestern Olympic Peninsula, Washington: U.S. Geological Survey Professional Paper 1162-B, 28 p.
- Tabor, R. W., and Cady, W. M., 1978a, Geologic map of the Olympic Peninsula area: U.S. Geological Survey Map 1-994, scale 1:125,000.
- 1978b, The structure of the Olympic Mountains, Washington—Analysis of a subduction zone: U.S. Geological Survey Professional Paper 1033, 38 p.
- Thiede, J., and Dinkelmann, M. G., 1977, Occurrence of *Inoceramus* remains in late Mesozoic pelagic and hemipelagic sediments, in Supko, P. R., Perch-Nielsen, K., and others, eds., Initial reports of the Deep Sea Drilling Project (Volume 39): Washington, D.C., U.S. Government Printing Office, p. 899-910.
- Thompson, A. B., 1971, PCO_2 in low-grade metamorphism: zeolite, carbonate, clay mineral, prehnite relations in the system $CaO-Al_2O_3-SiO_2-H_2O$: Contributions to Mineralogy and Petrology, v. 33, p. 145-161.
- Tiffin, D. L., and Riddihough, R. P., 1977, Gravity and magnetic survey off Vancouver Island, 1975: Geological Survey of Canada Paper 77-1A, p. 311-314.
- Tiffin, D. L., Cameron, B.E.B., and Murray, J. W., 1972, Tectonics and depositional history of the continental margin off Vancouver Island, British Columbia: Canadian Journal of Earth Sciences, v. 9, p. 280-296.
- Underwood, M. B., 1984, A sedimentologic perspective on stratal disruption within sandstone-rich mélange terranes: Journal of Geology, v. 92, p. 369-385.
- Wells, R. E., Engebretson, D. C., Snavely, P. D., Jr., and Coe, R. S., 1984, Cenozoic plate motions and the volcanic-tectonic evolution of western Oregon and Washington: Tectonics, v. 3, p. 275-294.
- Wood, D. M., 1982, Laboratory investigations of the behavior of soils under cyclic loading: A review, in Pande, G. N., and Zienkiewicz, O. C., eds., Soil mechanics—Transient and cyclic loads: New York, John Wiley and Sons, p. 513-582.

MANUSCRIPT RECEIVED BY THE SOCIETY APRIL 29, 1985

REVISED MANUSCRIPT RECEIVED JUNE 7, 1989

MANUSCRIPT ACCEPTED JUNE 12, 1989